

# **SAMS Acceleration Measurements on Mir from March to September 1996**

July 14, 1997

Milton E. Moskowitz  
Tal-Cut Company  
North Olmsted, Ohio

Ken Hrovat  
Tal-Cut Company  
North Olmsted, Ohio

Duc Truong  
NASA Lewis Research Center  
Cleveland, Ohio

Timothy Reckart  
Tal-Cut Company  
North Olmsted, Ohio

## Abstract

During NASA Increment 2 (March to September 1996), over 15 gigabytes of acceleration data were collected by the Space Acceleration Measurement System (SAMS) onboard the Russian Space Station, Mir. The data were recorded on 55 optical disks and were returned to Earth on STS-79. During this time, SAMS data were collected in the Kristall and Kvant modules, and in the Priroda module to support the following experiments: the Queen's University Experiments in Liquid Diffusion (QUELD), the Technological Evaluation of the MIM (TEM), the Forced Flow Flame Spreading Test (FFFT), and Candle Flames in Microgravity (CFM). This report points out some of the salient features of the microgravity environment to which these experiments were exposed. Also documented are mission events of interest such as the docked phase of STS-76 operations, an extravehicular activity (EVA) to install and deploy solar panels on the Kvant module, a Progress engine burn to raise Mir's altitude, and an on-orbit SAMS calibration procedure. Also included are a description of the Mir module orientations, and the panel notations within the modules. This report presents an overview of the SAMS acceleration measurements recorded by 10 Hz and 100 Hz sensor heads. Variations in the acceleration environment caused by unique activities such as crew exercise and life-support fans are presented. The analyses included herein complement those presented in previous mission summary reports published by the Principal Investigator Microgravity Services (PIMS) group.

# Abbreviations and Acronyms

A/D	Analog to Digital
BKV-3	dehumidifier (Russian acronym)
CFM	Candle Flames in Microgravity
dB	decibel
DMT	Decreed Moscow Time (year day/hour:minute:second)
EVA	extravehicular activity
$f_c$	cutoff frequency
FFFT	Forced Flow Flame Spreading Test
$f_N$	Nyquist frequency
$g_o$	Acceleration due to Earth's gravity at sea-level (9.81 m/s <sup>2</sup> )
Hz	Hertz
JSC	NASA Johnson Space Center
LeRC	NASA Lewis Research Center
LSLE R/F	Life Sciences Laboratory Equipment Refrigerator/Freezer
$\mu g$	microgravity (1/1,000,000 of $g_o$ )
mg	milligravity (1/1000 of $g_o$ )
MGBX	Microgravity Glovebox
MIM	Microgravity Isolation Mount
MiPS	Mir Payload Support
MRD	Microgravity Research Division
PIMS	Principal Investigator Microgravity Services
POSA	Payload Operations Support Area
PSD	power spectral density
QUELD	Queen's University Experiments in Liquid Diffusion
RMS	root-mean-square
RSS	root sum of square
rpm	revolutions per minute
SAMS	Space Acceleration Measurement System
STS	Space Transportation System
TDRSS	Tracking and Data Relay Satellite System
TEM	Technological Evaluation of the MIM
TSH	triaxial sensor head
USML-1	first United States Microgravity Laboratory
WORM	write once read many
WWW	world wide web
$X_h, Y_h, Z_h$	X-, Y-, Z-Axis for unspecified SAMS sensor head.
$X_{h,A}, Y_{h,A}, Z_{h,A}$	X-, Y-, Z-Axis for SAMS TSH A
$X_{h,B}, Y_{h,B}, Z_{h,B}$	X-, Y-, Z-Axis for SAMS TSH B
$X_B, Y_B, Z_B$	X-, Y-, Z-Axis coordinate system for Mir Base Block.

## Table of Contents

Abstract.....	i
Abbreviations and Acronyms .....	ii
Table of Contents .....	iii
List of Tables .....	iv
List of Figures.....	iv
Acknowledgements.....	v
1. Introduction and Purpose.....	1
2. Data Acquisition and Processing .....	2
3. Mission Configuration .....	3
3.1 Mir Configuration.....	3
3.2 Mir Coordinate Systems .....	3
3.3 Mir Panel Notation .....	4
3.4 Mir Attitudes.....	4
4. Triaxial Sensor Head Orientation and Location .....	4
5. Data Analysis Techniques.....	5
6. Mission Activities .....	5
6.1 Microgravity Isolation Mount (MIM) .....	5
6.2 Queen's University Experiments in Liquid Diffusion (QUELD) .....	6
6.3 Technological Evaluation of the MIM (TEM).....	7
6.4 Forced Flow Flame Spreading Test (FFFT).....	8
6.5 Candle Flames in Microgravity (CFM) .....	9
6.6 Extravehicular Activity (EVA) for Solar Panel Deploy .....	10
6.7 Progress Engine Burn .....	11
6.8 SAMS Calibration .....	11
6.9 Mir/Shuttle (STS-76) Docked .....	13
7. Mir Structural Modes.....	14
8. Equipment Operation.....	14
8.1 BKV-3 Compressor.....	14
8.2 Gyrodynes.....	15
8.3 Exercise Device Characteristics .....	16
8.4 Life-Support.....	17
9. Summary.....	19
10. References .....	21
Appendices	
A. Accessing Acceleration Data via the Internet .....	A1
B. SAMS Color Spectrograms for TSH A.....	B1
C. SAMS Color Spectrograms for TSH B.....	C1
D. User Comment Sheet .....	D1

### List of Tables

Table 1. Tabular representation of Mir module orientations.....	3
Table 2. Compilation of SAMS Sensor head locations and orientations for various times during NASA Increment 2.....	5
Table 3. EVA Activity Log (24-25 May 1996) .....	10
Table 4. Summary of possible SAMS calibration orientations.....	12
Table 5. SAMS Calibration data, taken in Priroda around DMT 169/14:47 .....	13
Table 6. Summary of $\mu g_{RMS}$ levels measured in Kvant due to BKV-3 compressor.....	15
Table 7. $\mu g_{RMS}$ levels from the life-support systems (primary frequencies), measured in the Kvant module .....	18
Table 8. $\mu g_{RMS}$ levels from the life-support systems (primary frequencies), measured in the Priroda module .....	19

### List of Figures

Figure 1. Typical Mir configuration with docked Orbiter .....	23
Figure 2. Mir module orientations .....	24
Figure 3. Compilation of PSDs of SAMS data acquired during MIM verification tests.....	25
Figure 4. Compilation of PSDs of SAMS data acquired during QUELD experiments, with and without the use of MIM .....	26
Figure 5. Compilation of PSDs of SAMS data comparing TEM and MIM verification tests of SAMS data.....	27
Figure 6. Compilation of PSDs of SAMS data acquired during FFFT experiments .....	28
Figure 7. Spectrogram of SAMS data acquired during an FFFT experiment .....	29
Figure 8. Time history of SAMS data acquired during a CFM experiment .....	30
Figure 9. Time history of SAMS data acquired during a crew sleep period .....	31
Figure 10. Spectrogram of TSH A SAMS data collected during an EVA to deploy solar panels .....	32
Figure 11. Spectrogram of TSH B SAMS data collected during an EVA to deploy solar panels .....	33
Figure 12. Time history of TSH A SAMS data showing the acceleration effects of a Progress engine burn .....	34
Figure 13. Time history of TSH B SAMS data showing the acceleration effects of a Progress engine burn .....	35
Figure 14. Power Spectral Density of SAMS TSH A data collected during the Progress engine burn event .....	36
Figure 15. Time history of SAMS TSH A data showing an on-orbit SAMS calibration activity .....	37
Figure 16. Spectrogram of TSH B SAMS data showing the microgravity environment of the Mir/Atlantis (STS-76) complex.....	38
Figure 17. Power Spectral Density of SAMS TSH A data showing BKV-3 frequencies.....	39
Figure 18. Spectrogram of TSH A SAMS data showing a gyrodyne spin-down activity .....	40
Figure 19. Spectrogram of SAMS TSH A data collected during a crew exercise period.....	41

Figure 20. Power Spectral Density of SAMS TSH A data showing frequencies related to the life-support systems in the Kvant module .....	42
Figure 21. Spectrogram of SAMS TSH A showing frequencies related to life-support systems in the Kvant module.....	43

### Acknowledgments

The authors would like to acknowledge a number of people who contributed time and effort to provide information which was used in this report. We would like to acknowledge the SAMS group (NASA LeRC) for providing the hardware, and for their processing the data from the optical disks to engineering units. Shannon Lucid performed an exceptional job of operating the SAMS unit, as well as keeping a logbook of some significant acceleration events which occurred during her stay on Mir. The NASA JSC POSA group's daily summaries proved to be an invaluable tool for our analysis of this data. Dr. Stanislav Ryaboukha (RSC/Energia) has once again proved to be a very important asset, given his knowledge of the Mir station and much of the onboard equipment. Gene Liberman and Katherine Chirokova were invaluable for their Russian-to-English skills (both verbal and written). Without these translation skills, Dr. Ryaboukha's knowledge base would have been for naught. Finally, we would like to thank Julio Acevedo (NASA LeRC, SAMS-Mir Project Manager) for his continuing efforts to keep SAMS recording on Mir, and for insuring that PIMS has access to the Russian experts.

## 1. Introduction and Purpose

The NASA Microgravity Research Division (MRD) sponsors science experiments on a variety of microgravity carriers, including Orbiter missions and the Russian Space Station, Mir. The MRD sponsors the Space Acceleration Measurement System (SAMS) at the NASA Lewis Research Center (LeRC) to support these science experiments by providing acceleration measurements to characterize the microgravity environment to which the experiments were exposed. The LeRC Principal Investigator Microgravity Services (PIMS) project supports principal investigators of microgravity science experiments as they evaluate the effects of varying acceleration levels on their experiments.

In 1994, a SAMS unit was installed on the Mir Space Station. In a manner similar to Orbiter mission support, the SAMS unit supports science experiments from the U.S. and Russia by measuring the microgravity environment during experiment operations. Previous reports [1-4] have summarized the SAMS data acquired during the period from October 1994 to March 1996.

During the time period from March to September 1996, SAMS supported several microgravity experiments by measuring the acceleration environment aboard the station. Some of these experiments are described below:

- The Microgravity Isolation Mount (MIM) is a platform which was developed to help isolate an experiment from the vibrational environment of an orbital laboratory. Additionally, the MIM may be used to impart controlled accelerations into the local environment, resulting in a pre-defined acceleration environment to the experiment on the MIM platform.
- The Technical Evaluation of MIM (TEM) experiment was designed to evaluate the performance of the MIM facility.
- The Queen's University Experiments in Liquid Diffusion (QUELD) allowed scientists to conduct experiments to determine the diffusion coefficients of metal and semiconductor materials.
- The Forced Flow Flame Spreading Test (FFFT) studied the effects of low-speed flow rate and bulk fuel temperature on combustion in a reduced gravity environment.
- The Candle Flames in Microgravity (CFM) experiment studied the behavior of candle flames in microgravity.

Also included in this report are some events of interest, including an analysis of the microgravity environment during the STS-76 docked phase operations, an extravehicular activity (EVA) to deploy solar panels on the Kvant module, a Progress engine burn, and an analysis of an on-orbit SAMS calibration procedure.

Appendix A describes how to access SAMS data, and SAMS and PIMS information over the internet. Appendix B provides color spectrogram plots of SAMS TSH A ( $f_c=100$  Hz) data. Appendix C provides color spectrogram plots of SAMS TSH B ( $f_c=10$  Hz) data. Appendix D contains a user comment sheet. Users are encouraged to complete this form and return it to the authors.

## 2. Data Acquisition and Processing

As previously reported [1-4], the SAMS unit on Mir simultaneously records data from two remote triaxial sensor heads (TSHs). The first head (denoted TSH A) utilizes a 100 Hz anti-alias lowpass filter, and digitizes (samples) data at a rate of 500 samples per second. The second head (denoted TSH B) utilizes a 10 Hz anti-alias lowpass filter, and digitizes data at a rate of 50 samples per second. The filter used for both sensor heads has a roll-off of -140 decibels (dB) per decade.

After this data filtering and sampling operation, the data are recorded onto optical WORM (Write Once Read Many) discs. The SAMS unit has two of these devices, and the storage capacity is 200 MB per disc side, for 400 MB total. Each disc may hold approximately 24 hours worth of data (12 hours per side).

The optical data discs are returned to Earth via the Space Shuttle, and are processed by the SAMS group at the NASA Lewis Research Center (Cleveland, Ohio). The processing of the data compensates for the temperature dependence of bias, scale factor, and axial misalignment considerations. The data are converted to engineering units of g, where 1 g is equal to the nominal Earth gravity of  $9.81 \text{ m/s}^2$ .

If the Mir Payload Support (MiPS) time synchronization was successful, then the timestamp used for the data is that received from the MiPS unit. If synchronization was unsuccessful, then the SAMS group relies on the crew member's logbook to determine the start time for data recording. In either case, the data is reported in Decreed Moscow Time (DMT). Depending upon the accuracy of the crew member's times listed in the logbooks (or the correction to the MiPS time notated by the crew), the timestamps of the SAMS data may be off from actual DMT by up to two days (typically, time gaps of a few minutes to an hour or two are seen). Further work to determine actual time is required, such as trying to compare timelines of known events with the accelerometer data.

Once the data are converted from the optical disc format to engineering units of g, the data are placed on the LeRC anonymous FTP server [beech.lerc.nasa.gov](http://beech.lerc.nasa.gov). Instructions for data access are listed in Appendix A of this report.



### 3. Mission Configuration

#### 3.1 Mir Configuration

The Mir Space Station was launched in 1986 as a base module and has been expanded since that time to include six modules as of 1996. Figure 1 shows the typical configuration of the Mir Space Station during the time covered by this report. The six major components are the Mir Core Module (living quarters, life-support, and power), the Kvant module (astrophysics instruments, life-support and attitude control equipment), the Kvant-2 module (biological research, Earth observation, and an airlock for EVA capability), the Kristall module (scientific equipment, retractable solar arrays, and a docking node), the Spektr laboratory module (Earth observation, specifically natural resources and atmosphere), and the Priroda module (remote sensing of Earth and hardware/supplies for several joint U.S.-Russian science experiments). The Mir modules are occasionally reoriented for mission activities such as vehicle docking events. The overall space complex mass exceeds 100 tons. The length along the longitudinal axis is about 33 meters (about 26 meters without the Progress module) and the length along the lateral axis is about 27 meters.

#### 3.2 Mir Coordinate Systems

The generic coordinate system of the Mir Space Station is that of the Mir Core Module. Each of the modules of the Mir station has its own coordinate system, which is based upon its orientation with respect to the Mir Core Module. The determination of the coordinate system is made by a simple procedure. If you "stand" in any module, such that your feet are on the floor, and you are facing towards the transitional node of the Base Block, then the coordinate system of that module is defined by the right hand rule, such that the direction you are facing is  $+X_{\text{module}}$ , the direction from your feet to your head is  $+Y_{\text{module}}$ , and the direction from your left to right is  $+Z_{\text{module}}$ . Figure 2 shows a graphical representation of these coordinate systems for the nominal Mir configuration (consistent with that shown in Figure 1). Table 1 shows a tabular representation of Figure 2.

**Table 1: Tabular representation of Mir module orientations**

<i>Base</i>	<i>Kristall</i>	<i>Kvant</i>	<i>Kvant-2</i>	<i>Priroda</i>	<i>Spektr</i>
$+X_B$	$+Z_{\text{Kristall}}$	$-X_{\text{Kvant}}$	$+Y_{\text{Kvant-2}}$	$-Z_{\text{Priroda}}$	$-Y_{\text{Spektr}}$
$+Y_B$	$-Y_{\text{Kristall}}$	$+Y_{\text{Kvant}}$	$-X_{\text{Kvant-2}}$	$-Y_{\text{Priroda}}$	$+X_{\text{Spektr}}$
$+Z_B$	$+X_{\text{Kristall}}$	$-Z_{\text{Kvant}}$	$+Z_{\text{Kvant-2}}$	$-X_{\text{Priroda}}$	$+Z_{\text{Spektr}}$

As an example of how to correlate Table 1 and Figure 2, consider the Priroda module. For this module,  $+X_{\text{Priroda}}$  corresponds with  $-Z_B$ ,  $+Y_{\text{Priroda}}$  corresponds with  $-Y_B$ , and  $+Z_{\text{Priroda}}$  corresponds with  $-X_B$ . Both Table 1 and Figure 2 may be used to compare the coordinate systems of a module with the Base, or a module with all the other modules.

### 3.3 Mir Panel Notation

Within each module (when facing oriented such that the right hand rule as specified in section 3.2 applies) there is a numbering system for the panels. Each panel is given a three digit designation, beginning with 1, 2, 3, or 4. These numbers are determined such that the 1xx panels are on the floor, the 2xx panels are along the left wall, the 3xx panels are on the ceiling, and the 4xx panels are along the right wall.

### 3.4 Mir Attitudes

The orientation attitudes of Mir during the March to September 1996 time period were not known at the time of this writing.

The Mir Space Station periodically corrects its attitude. This is accomplished by turning station-keeping gyroscopes off and using thrusters to establish the desired attitude. When the new attitude is established, the gyroscopes are turned on again. The exact meaning of gyroscope “turn off” is not clear, but it is believed that it refers to disengaging a clutch mechanism and does not mean stopping the gyroscope rotation.

## 4. Triaxial Sensor Head Orientation and Location

The SAMS TSHs are mounted to a structure or an experiment in a predetermined manner. The orientation of the TSH axes relative to the vehicle is measured and recorded for later use in analyzing the acceleration data. Using this information, the measured acceleration levels may be transformed to other orientations, such as an experiment-based coordinate system or the Mir coordinate system. The data is presented in the SAMS coordinate system for this report.

The determination of SAMS sensor head locations and orientations is made from a number of sources, including [5-8]. Often times, the dates are contradictory, especially when the sources refer to a planned move of SAMS, without verification that the move actually occurred. Ultimately, it is possible that the mounting of the sensor heads was not performed according to the plans.

A compilation of the best information currently available is presented in Table 2. This table lists the data start times in a new location. Since the movement of SAMS throughout Mir is sketchy (i.e. the actual date of a move), presentation with respect to data start times is more appropriate. In order to read this table, data from DMT day 115 (falling after DMT 084, but before DMT 117) would be recorded at the DMT day 084 location (Kristall module).

**Table 2: Compilation of SAMS Sensor head locations and orientations for various times during NASA Increment 2**

<i>Date</i>	<i>DMT 1996 Day</i>	<i>Module</i>	<i>TSH A</i>	<i>TSH B</i>
24 March 1996	084	Kristall	100 Plane $X_{h,A} = -Y_{\text{Kristall}}$ $Y_{h,A} = -X_{\text{Kristall}}$ $Z_{h,A} = -Z_{\text{Kristall}}$	100 Plane $X_{h,B} = -Y_{\text{Kristall}}$ $Y_{h,B} = +X_{\text{Kristall}}$ $Z_{h,B} = +Z_{\text{Kristall}}$
26 April 1996	117	Kvant	Panel 210 $X_{h,A} = -X_{\text{Kvant}}$ $Y_{h,A} = -Y_{\text{Kvant}}$ $Z_{h,A} = +Z_{\text{Kvant}}$	Panel 414 $X_{h,B} = +Z_{\text{Kvant}}$ $Y_{h,B} = +Y_{\text{Kvant}}$ $Z_{h,B} = +X_{\text{Kvant}}$
17 June 1996	169	Priroda	MIM $X_{h,A} = +Z_{\text{Priroda}}$ $Y_{h,A} = +X_{\text{Priroda}}$ $Z_{h,A} = +Y_{\text{Priroda}}$	MGBX $X_{h,B} = +Y_{\text{Priroda}}$ $Y_{h,B} = -X_{\text{Priroda}}$ $Z_{h,B} = +Z_{\text{Priroda}}$

## 5. Data Analysis Techniques

The SAMS data were examined using acceleration versus time, power spectral density (PSD) versus frequency, and spectrogram (PSD versus frequency versus time) techniques. Each of these techniques highlights different features contained in the data.

The PSD calculations are typically used to examine the frequency content of short periods of data (on the order of minutes worth of data). The PSD techniques used by PIMS are described in [9].

The spectrograms are used to show how the microgravity environment varies in intensity with respect to both the time and frequency domains. The spectrogram technique is explained in [9]. The spectrograms serve as a roadmap to the data for identifying the activities which occurred.

## 6. Mission Activities

### 6.1 Microgravity Isolation Mount (MIM)

Orbiting spacecraft such as the Mir Space Station are in a constant state of free-fall. In the ideal, this platform would provide a laboratory for conducting experiments in complete weightlessness. However, as one might expect, there are numerous vibratory sources that disturb this weightless environment. These disturbance sources originate from the operation of onboard equipment such as compressors, fans, pumps, thrusters, and so on. In addition, movement of the crew, especially during exercise, has a deleterious impact on the microgravity environment. Quasi-steady accelerations arising from

atmospheric drag, gravity gradient effects, and rotational forces disturb the microgravity environment below about 0.01 Hz. While these disturbances may be relatively small, they can produce undesirable effects on the scientific experiments.

The Microgravity Isolation Mount (MIM) was designed to attenuate oscillatory disturbances in the frequency range 0.01 to 100 Hz. MIM is a six degree of freedom magnetic levitation vibration isolation system that consists of three major components: a stator fixed to the station, a flotor which floats relative to stator, and a control unit. It also houses cooling fans to remove heat from the locker compartment. Experiments are mounted on the flotor, which is controlled by the control unit. MIM can operate in one of various modes: passive isolation based on position sensing, active operation of the magnetic suspension system, or an active mode that can excite an experiment with controlled oscillations in the 0.01 to 30 Hz frequency range [10]. MIM operational verification runs were conducted on DMT 1996 days 243, 244, and 253. The spectra shown in Figure 3 are representative of the microgravity environment on the locker door of MIM during its operation. The most prominent feature to note from the spectra in this figure is the train of peaks in the frequency range from 56 to 97 Hz, particularly on the  $Y_{h,A}$ -axis. In that region, there is a distinct peak at every Hertz or so from about 56 Hz up to about 97 Hz. These can also be seen to a lesser extent on the  $X_{h,A}$ - and  $Z_{h,A}$ -axes. The spectrogram in Figure 140 on page B-175 shows these distinctive peaks as a function of time. Note the dark red horizontal streaks in this figure, most noticeable above 60 Hz or so, which are relatively constant in frequency as a function of time. The source of this distinctive spectral signature is as yet unknown. During these MIM verification runs, structural modes dominated the spectra below 10 Hz. The BKV-3 compressor at about 24.2 Hz (along with its 2<sup>nd</sup>, 3<sup>rd</sup>, and 4<sup>th</sup> harmonics) and other life-support equipment in the 40 to 50 Hz range and in the 80 to 90 Hz range are other key acceleration contributors.

PIMS has proposed a tentative plan to the Canadian Space Agency and RSC-Energia to investigate these strong disturbances during Mir Increment 5 (May to September 1997).

## 6.2 Queen's University Experiments in Liquid Diffusion (QUELD)

During Shannon Lucid's stay aboard Mir, she conducted more than 40 materials processing experiment runs in the QUELD (Queen's University Experiments in Liquid Diffusion) furnace [11]. These experiments involved heating and mixing 55 combinations of metal and semiconductor materials. Each combination was encased in a sealed, pencil-sized sheath and heated in a special furnace roughly the size of a shoe box. The QUELD furnace, which can generate temperatures of up to 900°C, heats the specimens to molten temperature. The specimens are allowed to diffuse in this molten state and are then rapidly cooled so their final state can be returned to Earth for detailed analysis. The determination of metal diffusion coefficients is important for a variety of industrial processes including the development of new alloys and semiconductor materials. These experiments were performed in a microgravity environment in order to remove the effects of buoyancy, which dominate in an Earth-based laboratory. Despite the reduced-gravity environment achieved in the free-falling laboratory provided by Mir, equipment operation and crew movement contribute to g-jitter which may upset the diffusion process. To further isolate these sensitive experiments from vibratory disturbances such as these, the QUELD furnace was housed on the MIM.

According to [6], QUELD experiments were conducted on at least 17 days during the time frame ranging from DMT 1996 day 179 to day 240. It was noted that MIM was not operating for all of the QUELD runs on DMT 1996 day 187. When MIM was operating, the acceleration spectrum changed considerably relative to times when it was not operating. Figure 4 shows the spectral average of PSDs from a number of time periods spanning DMT 1996 day 179 to day 240. As seen in this figure, QUELD runs with MIM signature 1 (the red trace) display significant differences on the SAMS TSH A  $Y_h$ - and  $Z_h$ -axes when compared to QUELD runs with MIM signature 2 (the green trace). When MIM is operating so that signature 1 is observed, strong spectral components appear in the following frequency bands: 66 - 72 Hz, 73 - 80 Hz, 83 - 85 Hz, and 90 - 95 Hz at about every Hertz. Specifically, strong peaks occur at the following frequencies: 52.6, 53.6, 56.5, 57.5, 58.6, 66.7, 68.7, 69.6, 70.7, 72.5, 72.8, 73.7, 74.7, 75.6, 76.8, 77.8, 78.7, 79.7, 83.0, 84.0, 85.0, 87.9, 88.7, 89.0, 90.1, 90.9, 91.9, 92.8, 93.8, 94.9, 96.7, 97.9, and 98.9 Hz. The sources for these disturbances are not yet known, and this issue is still under investigation. Strong spectral contributors noted during QUELD runs, regardless of MIM operation, originate from the BKV-3 compressor at about 24.2 Hz (along with its 2<sup>nd</sup>, 3<sup>rd</sup>, and 4<sup>th</sup> harmonics), life-support equipment in the 40 to 50 Hz range (including a fan at 41 Hz), unknown disturbances in the 60 to 65 Hz range which are somewhat variable in frequency, and life-support equipment in the 80 to 90 Hz range.

### 6.3 Technological Evaluation of the MIM (TEM)

The Technological Evaluation of the MIM (TEM) is a fluid physics experiment that was developed with three primary objectives: (1) to show the effects of g-jitter on free surface oscillations in microgravity, (2) to evaluate the ability of the MIM to isolate the fluid physics experiment payload from these effects, and (3) to gather information on free surface response to a controlled g-jitter environment provided by the MIM [12]. The TEM hardware includes two mating assemblies: a baseplate and a test vessel that contains a 3 cm diameter cylinder, which is partly filled with liquid. These are mounted to the flotor of the MIM for experiment runs. The fluid system parameters for this experiment were chosen such that the natural frequencies of the free surface would be excited by the ambient microgravity environment of Mir [13]. This provided the proper scenario for the test objectives stated above. The free surface response to the unisolated Mir environment, the MIM-isolated environment, and the MIM-controlled environment was recorded on video for correlation to acceleration data collected on the MIM. This data was unavailable for comparison at the time this report was written.

According to the [6] and [7], the TEM experiment runs performed by Shannon Lucid from July to August of 1996 were conducted on DMT 1996 days 195, 197 – 200, and 244. Since the hardware that comprises TEM does not contain any components that would induce sustained vibrations (i.e. rotating machinery), one would expect the local microgravity environment measured on the MIM facility during TEM runs to be similar to those observed during the MIM verification runs. The plots shown in Figure 5 corroborate this for SAMS TSH A data collected from DMT 1996 197/20:00:00 to 197/20:04:22 and DMT 1996 253/14:40:00 to 253/14:44:22 for the MIM verification runs. As shown in Figure 5, the spectra match closely.

Exceptions to note are:

- the heightened response in MIM (red trace) data relative to the TEM (green trace) data for:
  - the 3.4 to 7.7 Hz range on the  $X_h$ -axis
  - the 7.4 to 11.3 Hz range on the  $Y_h$ - and  $Z_h$ -axes
  - the 75 to 95 Hz range on the  $X_h$ -axis
- the TEM peak at 40.4 Hz appears at 40.1 Hz for MIM
- the TEM peak at 49.2 Hz appears at 50.1 Hz for MIM on the  $Y_h$ -axis
- the TEM peak at 80.7 Hz appears at 81.8 Hz for MIM
- the TEM peaks at 86.7 Hz ( $X_h$ -axis) and 89.6 Hz ( $Z_h$ -axis) do not appear in the MIM data.

It is believed that the slight shifts in frequency for the two different time frames may be attributable to different loads on various life-support equipment [12] and [13].

#### 6.4 Forced Flow Flame Spreading Test (FFFT)

A primary physical mechanism in flame spreading is air movement through and around the flame. The motion of air provides oxygen, carries away combustion products, and controls how heat released from the flame is distributed [14]. On Earth, buoyant convection caused by gravity is the principal force for the movement of air. The FFFT was designed to study the effects of low-speed flow and bulk fuel temperature on flammability, ignition, flame growth, and flame-spreading behavior in the absence of buoyant convection. The microgravity environment of Mir affords this by providing a reduced-gravity environment, thus suppressing buoyancy forces. A related test was conducted during USML-1 (STS-50) where it was demonstrated that low-speed airflows could significantly increase the flammability of materials in microgravity. For tests conducted on Mir, the effects of varying fuel thickness and flow velocity on flames as they spread in a small, low-speed wind tunnel were observed. The temperature field in the fuel and in the flames was measured using thermocouple arrays, and the airflow was measured using a low-speed anemometer. A special video camera was also employed as part of the FFFT experiment to record and synchronize the spreading flames, the temperature displays, and the air flow measurements [15].

The FFFT experiment was conducted in the Microgravity Glovebox (MGBX) facility. The MGBX is a multi-purpose facility that provides a contained working volume designed to handle biological, fluids, combustion, and materials experiments involving small quantities of substances. For the FFFT experiment, the MGBX was used to prevent combustion products from contaminating Mir's atmosphere. FFFT test runs were conducted on 30, 31 July and 1 August 1996 (DMT 1996 days 212 – 214). During these runs, SAMS TSH B was mounted to the underside of the MGBX in the Priroda Module. Figure 6 shows PSDs calculated from the acceleration data recorded for the three orthogonal SAMS TSH B ( $f_c = 10$  Hz) axes during FFFT runs performed in the period from DMT 1996 212/14:20 to 212/18:20. From this data, it can be seen that much of the vibrational energy is concentrated in a relatively few number of narrow frequency bins in the 0.01 to 10 Hz range. To be more precise, a Mir structural mode at 1.1 Hz is evident on all three axes. Additionally, there are key components at 0.5, 0.9, 1.2, 1.4, and 3.7 Hz on the  $Y_{h,B}$ - and  $Z_{h,B}$ -axes. Exclusive to the  $Y_{h,B}$ -axis are spectral components at 2.2, 2.4, and 4.9 Hz, while there are 6.1, 7.3, and 8.0 Hz components seen only on the  $Z_{h,B}$ -axis. The background broadband energy in these PSDs is elevated by what appears to have been some considerable rattling

around the MGBX facility. This is evidenced by the numerous vertical red streaks in the color spectrogram shown in Figure 122 on page C-145. Comparing this spectrogram to the one shown for SAMS TSH A in Figure 99 on page B-117, we see that these impulsive events were localized to the SAMS TSH B location.

A primary concern for this experiment was the mass flow through the FFFT module [16]. A fan located in the outlet section of the test module controls this. An unequivocal determination of the operating times for this fan cannot be made due to the lack of detailed experiment timeline information. The operation of rotating machinery such as a fan can typically be detected in acceleration data, provided the rotational rate does not exceed the Nyquist frequency ( $f_N$ ) of the recorded data and there is sufficient transmissibility. The value of  $f_N$  for TSH B ( $f_N=62.5$  Hz) was most likely below the rotational rate of the fan. However, looking at SAMS TSH A ( $f_c = 100$  Hz,  $f_N = 250$  Hz) data recorded from DMT 1996 212/19:00 to 212/20:00 shown in Figure 7, there are well-defined disturbances at 43.4, 45.0, 46.6, and 48.2 Hz which run from about 6.5 to 25.5 minutes, from about 30.5 to 40.5 minutes, and from about 41.5 to 50.5 minutes in this plot. These disturbances are fairly tightly controlled in frequency and may have been caused by a fan. Note that SAMS TSH A was across the aisle from the MGBX facility in the Priroda module and while transmission of these vibrations through the surrounding structure may be possible, to attribute these disturbances to the MGBX facility would be speculation. The PIMS group continues to work with experiment teams and Russian colleagues to identify unknown disturbances such as these.

### 6.5 Candle Flames in Microgravity (CFM)

The CFM experiment was designed to study the behavior of candle flames in microgravity. In particular, this experiment studied how long flames can be sustained, the behavior of pre-extinction flame oscillations, and the behavior of two candle flames in close proximity. As stated earlier, while on Earth, buoyant convection is the dominant transport mechanism for flow around a flame. In a reduced-gravity environment, the transport of combustion products and oxygen occurs by the significantly slower process of molecular diffusion, which results when there is a concentration gradient within the candle flame. Simply stated, when there is a low concentration of oxygen and a high concentration of combustion products close to the flame, and a high concentration of oxygen and a low concentration of combustion products away from the flame, the combustion products migrate away from the flame and oxygen migrates toward the flame [17].

Shannon Lucid began CFM operations in the MGBX on 1 July 1996. Testing on Mir included 79 candle burns and was completed by 26 July 1996. According to [6,7], these experiments were run on DMT 1996 days 183 – 188, 194, 201, and 204 – 207. The CFM experiment houses an XY translation stage that holds two thermocouples to measure temperature in and around the candle flames. This hardware has potential for impacting the microgravity environment during candle burns, however, PIMS has been unable to find a source of information for how this equipment works, so identifying its operation in the acceleration data has not yet been accomplished. Also, after each candle test, the MGBX air circulation is turned on to supply fresh air to the glovebox and to filter out the combustion products [18]. It is believed that the MGBX circulation fans have a rotational rate above the Nyquist frequency of SAMS TSH B ( $f_c = 10$  Hz,  $f_N = 25$  Hz) and cannot be identified in the data for this sensor. The

environment measured by SAMS TSH B on the MGBX during CFM runs was marked by numerous, sporadic impulsive events that are perhaps attributable to crew activity at and around the MGBX facility. This is corroborated by a comparison of data recorded during CFM operations (see Figures 113 and 114 on pages C-134 and C-135) with data recorded during crew sleep (see Figure 115 on page C-136). The transient nature of the environment during CFM operations is clearly seen in Figure 8. In this figure, we see that the highest magnitude transient accelerations are on the  $X_{h,B}$ -axis. This corresponds to the  $Y_{Priroda}$ -axis. The acceleration vector magnitude during this time approached 1.5 mg. In stark contrast, compare this to crew sleep data shown in Figure 9. Note that the high magnitude transients are no longer present and the acceleration vector magnitude during this period did not exceed 70  $\mu$ g.

### 6.6 Extravehicular Activity (EVA) for Solar Panel Deploy

Around DMT 1996 145/23:47 (24 May 1996), the Mir Commander (Yuri Onufrienko) and Mir Flight Engineer (Yuri Usachyov) egressed from the Kvant-2 airlock to begin approximately 5 hours of extravehicular activity (EVA) in order to install and deploy solar arrays on the Kvant module. At the time of the data take, the SAMS unit was located in the Kvant module of the station.

Figure 15 in Appendix B shows a SAMS TSH A ( $f_c=100$  Hz) spectrogram for the majority of the crew EVA time. Comparison of this spectrogram with [6] yielded a number of timing coincidences. Table 3 shows a compilation of pertinent information from the 25 May 1996 POSA status report [6].

**Table 3: EVA Activity Log (24-25 May 1996)**

<i>DMT (year 1996)</i>	<i>Comment</i>
145/23:47	Hatch opening, egress (Kvant-2)
145/23:47 - 146/00:07	Translate to work site
146/00:07 - 146/00:22	Install 6 connectors
146/00:22 - 146/00:52	30 minute rest
146/02:15	Begin solar panel deploy
146/03:25	34 panels completed
146/04:14	Array fully deployed
146/04:40	Ingress

Comparison of these times with the plot in Appendix B will show an increase in the magnitude of the structural frequencies during periods of work. This is to be expected, as increased activity levels tend to increase the magnitude of the natural structural frequencies of the vehicle. Figure 10 shows a 1 hour time period from TSH A ( $f_c=100$  Hz), plotted to 10 Hz. Notice the increased magnitudes at  $t=11$  mins (and the subsequent decrease at  $t=51$  mins) of the 0.5, 1.1, 1.4, 2.1, 3.7, and 7.6 Hz modes. The starting time for this plot corresponds to a few minutes prior to the solar panel deploy operation. Figure 11 shows the plot for TSH B ( $f_c=10$  Hz) data for the same time period. Notice the similar character of these two data sets.



The solar panels were deployed using a hand crank, but no information was available as to the primary rotational frequency which might have been used by the cosmonauts. No spectral components have been identified in this plot which are believed to be related to this hand-crank frequency.

## 6.7 Progress Engine Burn

Periodically, the altitude of the Mir complex must be increased to counteract the aerodynamic drag which gradually reduces the altitude of the station. One method for such a procedure is to ignite the engines on one of the Progress vehicles docked to the station. The nominal life cycle for these Progress vehicles is to bring supplies from Earth to Mir, and then to return equipment, experiments, and trash from Mir to Earth.

During NASA Increment 2, Shannon Lucid noted in her log that a Progress engine burn was made around DMT 1996 184/12:00 (2 July 1996). When an engine burn such as this occurs, it is expected that there will be a temporary dc-level shift in the microgravity environment. An analysis of SAMS data from DMT 1996 184/11:45 to 184/11:50 has yielded the 0.25 second interval average plots shown in Figures 12 and 13 for TSH A ( $f_c=100$  Hz), and B ( $f_c=10$  Hz), respectively. In these figures, the data is presented in SAMS head coordinates for each of the sensors, so the coordinate systems do not match for the two sensors. Notice the approximate 2300  $\mu\text{g}$  dc shift from  $t=50$  to  $t=100$  seconds in Figures 12 ( $X_{h,A}$ -axis) and Figure 13 ( $Z_{h,B}$ -axis). It is believed that this 50 second offset spans the duration of the engine firing. When the coordinate transformations are taken into account (see Table 2), it may be seen that the primary thrust direction is in the  $+X_B$  direction. This implies a Progress vehicle docked to the Transitional Module (the spherical node to which the modules dock) where the Soyuz vehicle is shown in Figure 1.

During the engine firing event, a number of structural modes were excited. A PSD plot for TSH A ( $f_c=100$  Hz) data for a period contained entirely within the dc-shift region (DMT 1996 184/11:45:52 - 184/11:46:34) is shown in Figure 14. Notice the peaks below 4 Hz, including 0.19, 0.33, 0.61, 0.83, 1.07, 1.35, 1.58, 1.83, 2.10, 2.17, 2.57, 2.75, 2.87, 3.26, and 3.63 Hz.

The overall appearance of this plot is consistent for that observed during a similar event during the NASA Increment 3 dataset. However, the data from NASA Increment 3 showed that the burn occurred for a longer duration (about 6 minutes), but with a smaller dc-level shift (on the order of 400  $\mu\text{g}$ ).

## 6.8 SAMS Calibration

In order to achieve a better measure of the offset bias of the SAMS sensor heads, the Mir crew members have been asked to periodically perform a calibration procedure. This procedure is accomplished by two successive 180° rotations of the SAMS sensor head, once about the  $Z_h$ -axis, and then about the  $X_h$ -axis. This procedure results in three distinct periods of recorded data.

The primary assumption made is that the input signal (acceleration) is identical throughout the entire calibration procedure. If this is true, then by the use of two of the three periods, we can mathematically solve for the instrument's offset bias. This is accomplished by adding periods with opposite acceleration

inputs (for example, a period for which  $+X_h$  faced starboard, and then a period for which  $+X_h$  faced port) and dividing the result by 2. Since two rotations were performed (resulting in 3 data segments), each axis may be calibrated twice, using 2 of the 3 data segments. The calibration procedure is described in detail in [19].

The sensor heads are calibrated as close to their position of use as possible. Although directions such as “floor” and “ceiling” have less meaning in space, they are useful in describing the calibration procedure for this document. It should be noted that the sensor is not always calibrated using the floor and ceiling as reference frames, but they are the most helpful terms to use here. Table 4 shows a possible orientation for the sensor head for the three calibration segments (before and after each rotation). Since the sensor head rotations are always conducted using a predetermined sequence, Table 4 is always valid, even though the reference points (i.e. floor/ceiling, fore/aft, starboard/port) may not be accurate for each and every calibration period.

**Table 4: Summary of possible SAMS calibration orientations**

<i>Period</i>	<i><math>+X_h</math>-axis</i>	<i><math>+Y_h</math>-axis</i>	<i><math>+Z_h</math>-axis</i>
<i>1</i>	Floor	Aft	Port
<i>2</i>	Ceiling	Aft	Starboard
<i>3</i>	Ceiling	Fore	Port

By choosing two segments for a single axis which point the sensor in opposite directions, the quantity defined by half of the sum of the means of the periods is equal to the offset bias determined from that calibration. Stated mathematically, considering the  $X_h$ -axis data from period 1 ( $x_1$ ), and period 2 ( $x_2$ ):

$$\text{offset bias} = \frac{\bar{x}_1 + \bar{x}_2}{2}.$$

During the NASA Increment 2 data, the SAMS unit (TSH A) was calibrated in the Priroda module around DMT 1996 169/14:47 (17 June 1996). Figure 15 shows a plot of the SAMS data from TSH A, showing the data recorded during the calibration procedure. The two sets of spikes seen in the data were caused by the manual rotation and manipulation of the sensor head. The quieter periods between the spikes are the actual calibration periods, as described in Table 4. Analysis of the data yields Table 5.

**Table 5: SAMS Calibration data, taken in Priroda around DMT 169/14:47**

	<i>Period</i>			<i>Results of Offset Bias equation</i>		
<i>Axis</i>	1	2	3	1	2	Mean
<i>X</i>	14.4 $\mu\text{g}$	16.6 $\mu\text{g}$	15.1 $\mu\text{g}$	15.50 $\mu\text{g}$	14.75 $\mu\text{g}$	15.125 $\mu\text{g}$
<i>Y</i>	-88.9 $\mu\text{g}$	-91.6 $\mu\text{g}$	-87.0 $\mu\text{g}$	-87.95 $\mu\text{g}$	-89.30 $\mu\text{g}$	-88.625 $\mu\text{g}$
<i>Z</i>	-25.0 $\mu\text{g}$	-25.3 $\mu\text{g}$	-23.7 $\mu\text{g}$	-25.15 $\mu\text{g}$	-24.50 $\mu\text{g}$	-24.825 $\mu\text{g}$

As Table 5 shows in the results columns, the offset biases determined from the procedure are not identical for the two sets of opposing data from each axis, but are in agreement within a couple of micro-g's. The primary source of error within this procedure is the assumption that all of the periods will be of identical data input. Since the microgravity environment of an orbiting laboratory (such as Mir) is so dynamic, this assumption is not accurate. Therefore, SAMS data are de-measured prior to use, to avoid introducing offset bias uncertainties into further analysis.

### 6.9 Mir/Shuttle (STS-76) Docked

Previous PIMS Mission Summary Reports [3,4,20] have shown spectrogram plots of the microgravity environment during a Shuttle/Mir docking or undocking operation. During the docked phase of STS-76 operations, the SAMS unit was activated on Mir (we believe in the Kristall module), to record the microgravity environment of the Shuttle/Mir complex.

Figure 16 shows a color spectrogram of TSH B ( $f_c=10$  Hz) data for the time period DMT 1996 084/20:00 - 085/00:00 (24 March 1996). Note that although this sensor head utilized a 10 Hz lowpass filter, the data may still be plotted up to 25 Hz, the Nyquist frequency for this sensor. Care should be taken when analyzing figures plotted above the cutoff frequency, as the data above the cutoff have been attenuated by a -140 dB/decade filter, and thus will appear artificially low in magnitude (i.e. tend towards blue).

In Figure 16, notice the yellowish-green horizontal line around 17 Hz, and the on/off behavior of a cyan blue signal around 23-24 Hz, showing 7 active cycles during the time period contained within this plot. The 17 Hz line is the disturbance created by the dither of the Ku-band communication antenna on the Orbiter Atlantis. This antenna is dithered at a frequency of 17 Hz in order to prevent stiction, thus allowing the antenna to slew smoothly, in order to track the Tracking and Data Relay Satellite System (TDRSS). The 23-24 Hz disturbance was caused by the compressor on the Life Sciences Laboratory Equipment Refrigerator/Freezer (LSLE R/F) flown in the SPACEHAB module on Atlantis. The cyclic on/off behavior of this disturbance represents the on and off cycle of the refrigerator/freezer which was required to maintain the desired temperature. Compressor-on periods are identified by the presence of the 23-24 Hz cyan trace in Figure 16, while compressor-off periods are identified by the lack of this cyan trace. Since both of these disturbances lie above the cutoff frequency, accurate  $g_{\text{RMS}}$  information can not

be obtained from this data. Even without accurate  $g_{\text{RMS}}$  levels, it is still apparent that the vibrations caused by equipment operating aboard the Orbiter were transferred to the Mir station.

## 7. Mir Structural Modes

Any structure, including the Mir Space Station and all of its components, has natural frequencies (structural modes) characteristic of its underlying construction. These depend on many factors such as geometry, mass distribution, materials used in fabrication, and so forth. On Mir, the acceleration spectrum below about 10 Hz is dominated by structural mode vibrations, except during crew exercise. For the configuration shown in Figure 1 and the SAMS TSH B mounted on the MGBX in the Priroda Module, we see from Figures 75, 117, and 144 on pages C-89, C-138, and C-177, respectively, that Mir has measurable structural modes at about 0.5, 0.6, 0.9, 1.1, 1.4, 2.2, 3.6, 5.8, 6.4, and 7.5 Hz. Spectral peaks close to these values were also detected in the data for SAMS TSH A, which was mounted near the MIM in the Priroda Module. The spectral peaks at 1.1 and 1.4 Hz were the most intense, and the energy for those above 3 Hz was distributed over a broader bandwidth relative to the less diffuse, lower frequency modes. Transient and oscillatory disturbances, such as thruster firings and crew exercise, will excite these modes. For example, Figure 47 on page C-59 shows the structural response when a crew member is exercising. Note in particular, the increased intensity of the 0.5, 0.9, 1.1, and 2.2 Hz modes during the exercise period.

## 8. Equipment Operation

### 8.1 BKV-3 Compressor

The most intense disturbance recorded in the SAMS data from Mir is the 24 Hz signal, related to the operation of the BKV-3 compressor, which is housed in the Mir Core Module [5]. The microgravity disturbances caused by this system have been documented in the past by the French CNES [21] and the American SAMS [1-4] accelerometer systems. The function of this system is to compress and remove humidity from the Mir atmosphere. This unit had been in operation all of the time, but its use is now determined based upon the humidity levels aboard the station [5].

The fundamental frequency of this disturbance is nominally 24.4 Hz, however sub-frequencies (12.2, 6.1 Hz) have been recorded, as have upper harmonics of both the fundamental and the sub-frequencies (i.e. 36.6, 48.8 Hz). The fundamental frequency has been noted to float between 23.93 and 24.4 Hz. This floating, however, will only occur at quantized (discrete) frequencies, depending on the load of the system. The cause of the related 12.2 and 6.1 Hz signals is unknown, and these signals are not always present in the data. A detailed analysis (performed by the Russians) has shown that these 12.2 and 6.1 Hz signals do not exist within the BKV-3 compressor itself [5].

Table 6 summarizes the  $\mu g_{\text{RMS}}$  levels caused by the BKV-3, this data was recorded by SAMS TSH A ( $f_c=100$  Hz) in the Kvant module of the Mir station. The data represents the 10 minute period DMT

1996 125/09:00 - 125/09:10 (4 May 1996). A boxcar window was applied during data processing, and spectral averaging was performed, such that the frequency resolution was approximately 0.03 Hz.

**Table 6. Summary of  $\mu g_{RMS}$  levels measured in Kvant due to BKV-3 compressor**

			$\mu g_{RMS}$			
$f_{low}(Hz)$	$f_{mid}(Hz)$	$f_{high}(Hz)$	$X_{h,A}-Axis$	$Y_{h,A}-Axis$	$Z_{h,A}-Axis$	$RSS_{h,A}$
6.07	6.10	6.15	0.85	1.37	0.89	1.52
12.18	12.21	12.24	2.44	1.02	1.59	2.56
24.20	24.41	24.61	1613.9	1216.6	667.8	1740.4
36.40	36.63	36.83	109.4	53.84	12.85	111.0
48.64	48.83	48.98	283.9	289.0	159.0	344.7

As the above table shows, the primary frequency (24.4 Hz) is very tightly controlled in the frequency domain, and is a very loud ( $>1700 \mu g_{RMS}$ ) acceleration disturbance.

Figure 17 shows a plot of the Power Spectral Density (PSD) of the RSS combination of the three axes. Notice the 24.4 and 48.8 Hz peaks, and how tightly controlled they are in frequency, each orders of magnitude above the PSD level of the background accelerations around those frequencies.

An example of the quantized “floating” of the primary frequency may be seen in Figure 20, page B-26. In this figure, notice the “stair-step” behavior of the 24 Hz signal, as it increases just before DMT 1996 179/16:00, and then decreases back to its original level around DMT 1996 179/17:10.

Analysis of the SAMS data collected between May and July of 1996 (in the Kvant and Priroda modules) has shown that the compressor generally turns on in the morning (around 9am DMT), and turns off in the evening (around 6pm DMT). These times are approximate, and there are days with on and off activity which differ from what is listed above.

## 8.2 Gyrodynes

Each module of the Mir Station has at least one bank of 6 gyrodynes that are used to maintain station attitude. These operate at a nominal rotational rate of 10,000 rpm (approximately 166.7 Hz) and are normally tightly controlled in frequency. On occasion, one or more of these gyrodynes has to be spun-down. Figure 18 shows SAMS TSH A data recorded in the Kvant Module during such an activity. At around DMT 1996 124/17:22 (3 May 1996), at least one of the station’s gyrodynes began ramping down from its nominal 166.7 Hz rotational rate. This spin-down of the gyrodyne flywheel took approximately 3 hours and 15 minutes to complete. At first glance, the spin-down in frequency appears linear with respect to time, but closer inspection reveals that the slope gradually increases with time. Another gyrodyne spinning down at a somewhat faster rate can also be seen in Figure 18. Onset of spin-down for

this second trace is not pronounced, but assuming a constant slope, we can extrapolate that this second spin-down began at about DMT 1996 124/19:05 and took approximately 1 hour and 35 minutes to complete. The spectrogram shown in this figure is plotted to the Nyquist frequency (250 Hz) of the sensor head. The lowpass filter for this sensor head has a cutoff frequency of 100 Hz with a 140 dB per decade roll-off, so that the magnitude of the spectrum above 100 Hz has been attenuated. Despite this, note the trellis-like traces above 170 Hz between DMT 1996 124/18:20 and 124/20:00. These are attributable to signal aliasing and indicate that some strong components of the gyrodyne spin-down disturbance occur above the Nyquist frequency. In fact, at the 16th Microgravity Measurements Group Meeting, Stanislav Ryaboukha (RSC-Energia) noted that as the gyrodyne spin-down frequency decreases, it excites various structures at different frequencies. He could not provide specific structures or locations where this resonance occurred.

### 8.3 Exercise Device Characteristics

The Mir Space Station offers four exercise devices: 2 treadmills, and 2 Velo-ergometers. One of the treadmills is located in the Kristall Module, the other treadmill and a Velo-ergometer are located in the Mir Core Module, and the second Velo-ergometer is located in the Spektr Module. The Russian exercise protocol is setup such that the crew members rotate among the two different types of exercise, using each for 3 days at a time. Also, the crew has “expander” devices to use. These so-called expanders are spring-coil or bungee-type resistance exercise equipment, stretched by the crew member’s arms, and are used to build and/or maintain upper body muscle. These expanders are typically used in conjunction with either the treadmill or the Velo-ergometer. A typical treadmill exercise cycle may be to run, expand, run, expand, and so on.

Due to the lack of sufficiently detailed timeline information, the PIMS group has had problems trying to positively identify characteristics of acceleration disturbances caused by the two different types of exercise. Expander-type exercise is not expected to cause significant acceleration disturbances (compared with disturbances caused by either the treadmill or the Velo-ergometer). In the past, PIMS has been able to canvas disturbances caused by a number of exercise devices flown on the Orbiters: rowers, treadmills, and ergometers. Comparisons between these previously identified sources and what is believed to be exercise periods recorded on Mir have yielded a number of tentative identifications, each with some unknown characteristics. These unknown issues are being pursued with Russian scientists in order to accurately describe the Mir exercise environment.

Exercise recorded aboard the Orbiters has a much “cleaner” signal appearance. In this context, a “cleaner” signal refers to the signal being more tightly controlled in frequency. Perhaps the greatest cause for this difference between the two vehicles is the complexity and size of the Mir station, as opposed to the Orbiters. What is being measured is the acceleration response in the Priroda Module caused by exercise in either the Mir Core Module, the Kristall Module, or the Spektr Module. Since transmission of acceleration signals is a very complex phenomenon, little theoretical work has been done at this time to predict what the acceleration spectra is expected to look like, taking acceleration transmission from one module to another into account. The PIMS group will continue to work with Russian scientists in a continuing effort to characterize the microgravity environment of the Mir Space Station.

The treadmills may be used in either an active (motor-assisted), or passive (non-motor-assisted) mode. The motor-assisted mode has five discrete speed settings (which are unavailable to the authors at the time of report printing). In non-motor assisted mode, the astronaut/cosmonaut is free to run at their own pace. The characteristics of treadmill exercise (studied from previous Orbiter flights) show a very strong disturbance caused by the footfall of the crew member. Additionally, structural mode excitation has been observed.

The characteristics of ergometer exercise have been studied from previous Orbiter flights. Previous experience has shown that there should be a fundamental frequency in the 2-2.5 Hz region (related to the pedaling frequency), and a lower frequency of 1-1.25 Hz (related to the crew member's shoulders rocking back and forth as they pedal). Additionally, harmonics of these frequencies, and structural mode excitations are observed.

The identification of the two types of exercise aboard Mir has been very difficult due to a number of factors including the complexity of the Mir station (i.e. SAMS measurements have been made in modules other than where the ergometer is), the Russian exercise protocol (using the expanders between periods of other exercise), and a lack of accurate timeline information which show specific times for Velo-ergometer use. Despite these uncertainties, PIMS is readily able to identify exercise on Mir in general, but not treadmill or Velo-ergometer in particular.

Figure 19 shows a color spectrogram of SAMS TSH A ( $f_c=100$  Hz) data, plotted from 0-10 Hz, for clarity. Notice the (roughly) 2.5 Hz signal which occurs during the following times:  $t=23-29$  mins, 32-35 mins, 39-44 mins, and 46-53 mins. It is believed that this is related to exercise (either the pedaling rate for Velo-ergometer exercise, or the footfall rate for treadmill exercise). The periods between these "active" times has been tentatively identified as expander use (i.e. when the crew member would stop running/pedaling, and use the expander devices).

## 8.4 Life-Support

The Mir life-support systems are a complex series of fans, compressors, and controllers which all work together in order to sustain human existence aboard the space station. Frequencies in the 38-44 Hz region have been identified as being apart of the life-support systems [5]. In addition, harmonics of many of these frequencies (76-88 Hz) also appear in the SAMS data. Since the life-support systems need to function 24 hours a day, acceleration disturbances caused by these systems are always present in the data. Although the character of these signals sometimes looks different, the systems are always active.

Color spectrograms of SAMS TSH A data (see for example Figure 6 in Appendix B) show approximately 4 main traces (around 39.0, 39.6, 41.0, and 41.9 Hz). Figure 20 shows a power spectral density (PSD) plot of the 38-44 Hz region of the spectrum, recorded in the Kvant module from DMT 1996 125/08:00 - 125/08:10 (4 May 1996). This shows that there are more than just these four peaks in the frequency domain, believed to be caused by the life-support systems. The cause for the multiple, discrete peaks is unknown. One speculation for this behavior is that these could be contributions from any nearby fans and compressors. Another possible explanation is that these multiple peaks are

contributions from a single component, which is slightly variable in frequency, which manifest as multiple peaks due to the spectral averaging performed on this 10 minute data segment. The  $\mu g_{RMS}$  levels from these 4 primary frequencies are shown in Table 7.

**Table 7:  $\mu g_{RMS}$  levels from the life-support systems (primary frequencies) measured in the Kvant module**

$f_{lower} (Hz)$	$f_{upper} (Hz)$	$g_{RMS} (\mu g_{RMS})$
38.79	39.27	120.75
39.36	39.91	260.08
40.65	41.44	443.55
41.57	42.31	182.05

In addition to these frequencies, the Kvant module houses a series of vacuum valves, which are part of the overall life-support system for the entire Mir station. Although other modules have similar vacuum valves, they are used for a different purpose, and function in a different manner. The acceleration signature for these valves occurs in the 88-92 Hz region, seen quite clearly in SAMS TSH A data recorded in Kvant during the year 1995. A plot of data from DMT 1995 216/20:00 - 216/21:00 (4 August 1995) is shown in Figure 21. In this plot, notice the short, red, periodic, diagonal lines around the 90 Hz region. These are related to the cycling of this system. The periodicity of this disturbance has been seen to change, depending (among other things) on the number of crew members present. More recent data recorded in Kvant has not shown this disturbance. It has been speculated that this could be due to differences in sensor mounting, but no definite explanation for this lack of activity in more recent data has been confirmed.

The character of the life-support systems recorded in the Priroda module differs greatly from that recorded in the Kvant module. Table 8 lists some of the primary disturbance frequencies measured in the Priroda module from DMT 1996 182/08:00 - 182/08:10 (30 June 1996) which are believed to be caused by the life-support systems.



**Table 8:  $\mu g_{RMS}$  levels from the life-support systems (primary frequencies) measured in the Priroda module**

$f_{lower}(Hz)$	$f_{upper}(Hz)$	$g_{RMS} (\mu g_{RMS})$
39.92	40.49	1225.60
41.394	41.667	170.63
41.840	42.008	45.86
42.785	43.157	98.07
43.157	43.280	20.06
43.360	43.802	19.29
44.616	44.924	30.95

Although the Priroda module has a singular peak (around 40.23 Hz) which is significantly higher than any of the life-support peaks in the Kvant module, the remainder of the Priroda life-support frequencies are noticeably quieter than the levels measured by SAMS in Kvant.

## 9. Summary

The microgravity acceleration environment of a spacecraft in a low-Earth orbit is a very complex phenomenon. Many factors, such as experiment operation, crew activity, life-support systems, equipment operation, aerodynamic drag, gravity gradient and rotational effects, and structural resonance frequencies (structural modes) all contribute to form the overall microgravity environment. Distance along an acceleration transmission path is known to play an important role in defining the acceleration disturbance measured at one point in the vehicle, when the acceleration disturbance source originates at another point in the vehicle.

The Space Acceleration Measurement System (SAMS) on Mir utilizes two remote Triaxial Sensor Heads (TSHs) to measure the acceleration environment within the station. TSH A records data at 500 samples per second, with a 100 Hz lowpass anti-aliasing filter. TSH B records data at 50 samples per second, with a 10 Hz lowpass anti-aliasing filter. For most of the time, data is available for both sensor heads. Early in NASA Increment 2 (DMT 1996 days 084-119, 24 March - 28 April 1996) TSH A was disconnected, and only TSH B data is available.

SAMS data were recorded during NASA Increment 2 to support a number of facilities and experiments. Measurements on the Microgravity Isolation Mount (MIM) were made on the locker door, and are not indicative of the isolated environment. Results of SAMS data analysis have shown a number of regularly spaced spectral peaks (roughly every 1 Hz) from 56-97 Hz that appear to be related to MIM operations. Accelerometer data collected during the Technological Evaluation of the MIM (TEM) experiment show similar disturbances when compared with the MIM verification runs. SAMS data

collected during runs of the Queen's University Experiments in Liquid Diffusion (QUELD) showed two distinct acceleration signatures. These data support the conclusion that the locker door is subject to these distinctive induced accelerations while MIM is active. The cause for these disturbances is unknown, and still under investigation.

A structure such as the Mir Space Station has natural structural modes of vibration. These depend on a number of factors including geometry, mass distribution, and materials used for the fabrication of the structure. These structural modes are the primary disturbance source on Mir below about 10 Hz. Some common frequencies recorded in the Priroda module during NASA Increment 2 were 0.5, 0.6, 0.9, 1.1, 1.4, 2.2, 3.6, 5.8, 6.4, and 7.5 Hz. When an Orbiter is docked to Mir, some structural modes tend to shift, while others (related to the Orbiter) will show-up in SAMS data. This report showed a plot of SAMS data recorded on Mir for a period of time when Atlantis was docked (STS-76), which show these structural modes.

Life-support equipment needs to be operated continually in order to provide an environment which may sustain human existence in space. Primary frequencies in the 38.5-45 Hz region have been identified as the primary disturbances caused by some life-support equipment operation. In addition, harmonics of these frequencies (around 80 Hz) have been seen in SAMS data. Within the Base Block of Mir, there is a dehumidifier, designated the BKV-3, which operates with a nominal frequency of 24 Hz. This disturbance source has been measured in excess of  $1.5 \text{ mg}_{\text{RMS}}$ , and is perhaps the single largest disturbance source on the station.

Analysis of SAMS data recorded at the Microgravity Glovebox (MGBX) location has shown a large number of intense transients on spectrogram plots. It is believed that this appearance is related to crew activity in and around the MGBX facility while it is in operation. SAMS data from two MGBX experiments support this conclusion: the Forced Flow Flame Spreading Test (FFFT), and the Candle Flames in Microgravity (CFM) experiments.

An extravehicular activity (EVA) was performed during NASA Increment 2 in order to install and deploy arrays of solar panels outside the Kvant module. Analysis of SAMS data, and correlation with known times from the EVA event yielded a correspondence between structural mode excitation and lack of excitation with increased and decreased activity while the two cosmonauts were outside of the vehicle.

A Progress engine burn was shown to cause a dc-offset of approximately 2.3 mg for about 50 seconds. During this time frame, a number of modes below 4 Hz were excited. Data from both TSH A and TSH B showed that the primary direction of acceleration was  $+X_B$ . This is consistent with a Progress vehicle docked to the Transitional Module. Progress engine burns such as this are performed periodically in order to boost the altitude of the Mir station.

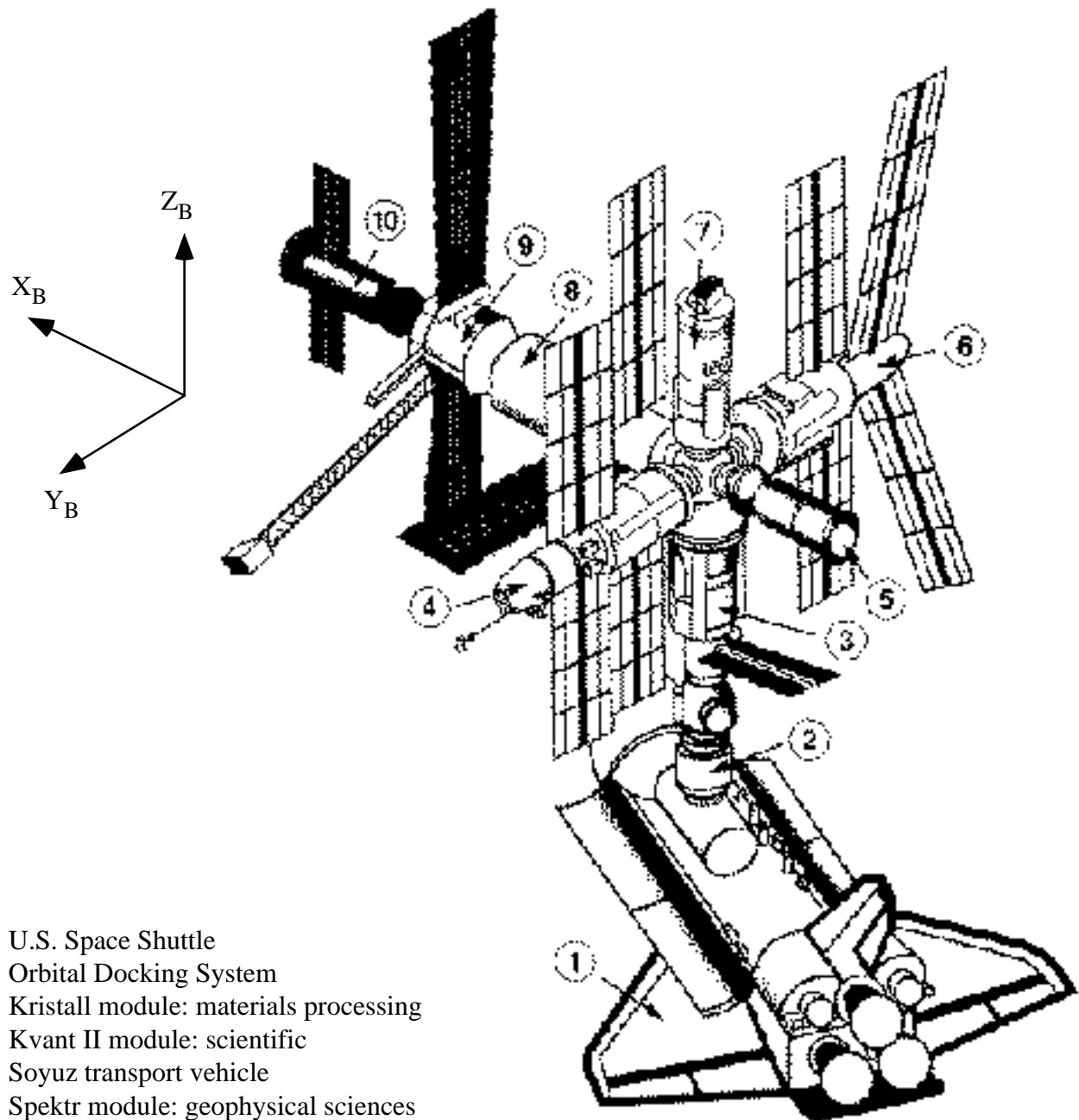
Gyrodynes are used to control the overall orientation of the Mir station. A bank of at least six gyrodynes are located within each module of the station. The nominal rotational rate of these is 10,000 rpm ( $\sim 166.6 \text{ Hz}$ ). Although above the filter cutoff for TSH A, these disturbances may be seen in SAMS data. Periodically, the gyrodynes need to be spun-down or spun-up. When this occurs, a color

spectrogram shows a frequency trace which originates at 166.6 Hz (for a spin-down) or 0 Hz (for a spin-up), and goes up or down, accordingly. The time period for this change has been shown to be roughly 3-4 hours.

## 10. References

- [1] DeLombard, R. and M. J. B. Rogers: Quick Look Report of Acceleration Measurements on Mir Space Station During Mir-16. TM-106835, January 1995.
- [2] DeLombard, R., S. B. Ryabukha, M. Moskowitz, K. Hrovat: Further Analysis of the Microgravity Environment on Mir Space Station During Mir-16. TM-107239, June 1996.
- [3] DeLombard, R., K. Hrovat, M. Moskowitz, K. McPherson: SAMS Acceleration Measurements on Mir From June to November 1995. TM-107312, September 1996.
- [4] DeLombard, R.: SAMS Acceleration Measurements on Mir From November 1995 to March 1996. TM-107435, April 1997.
- [5] Stanislav Ryaboukha, RSC-Energia, Personal communication.
- [6] JSC POSA Mir Status Report.
- [7] Shannon Lucid's SAMS notebook.
- [8] Julio Acevedo, SAMS-Mir Project Manager, personal communication.
- [9] <http://www.lerc.nasa.gov/WWW/MMA/PIMS/HTMLS/analysis.html>.
- [10] Tryggvason, B.V.: Microgravity Vibration Isolation Mount (MIM) Update on Mir Flight Test Program presented at the 15<sup>th</sup> MGMG Meeting, Kent, Washington, April 29 – May 1, 1996.
- [11] <http://www.science.sp-agency.ca/pub/queld-sep-25-96-e.html>.
- [12] Allen, J.S., and Harrison, M.E.: Liquid Surface Oscillations in a Microgravity Environment: Results of the TEM Experiment.
- [13] Dr. Roshanak Hakimzadeh, TEM Project Scientist, NASA LeRC, Personal communication.
- [14] <http://zeta.lerc.nasa.gov/EXPR2/FFFT-1.HTM>.
- [15] <http://mgnwww.larc.nasa.gov/fall96/fall96mfu.html#A.1.3>.

- [16] Kurt Sacksteder, MGBX Investigator (NASA LeRC), Personal communication.
- [17] <http://mgnwww.larc.nasa.gov/fall96/fall96mfu.html#A.1.2>.
- [18] <http://zeta.lerc.nasa.gov/expr/cfm.htm>.
- [19] SAMS - Space Acceleration Measurements System Flight Data Files, Section 9, Increment #2.
- [20] Rogers, M. J. B., M. Moskowitz, K. Hrovat, T. Reckart: Summary Report of Mission Acceleration Measurements for STS-79. CR-202325, March 1997.
- [21] Ryaboukha, S. B.: Characteristics of Main Sources of Vibration On Board Mir Station presented at the 16th MGMG Meeting, Gainesville, Florida, May 14 - May 16, 1997.



- 1) U.S. Space Shuttle
- 2) Orbital Docking System
- 3) Kristall module: materials processing
- 4) Kvant II module: scientific
- 5) Soyuz transport vehicle
- 6) Spektr module: geophysical sciences
- 7) Priroda Module: Earth remote sensing
- 8) Core module: habitation, power, life support
- 9) Kvant module: astrophysics
- 10) Progress vehicle

Figure 1. Typical Mir configuration with docked Orbiter.

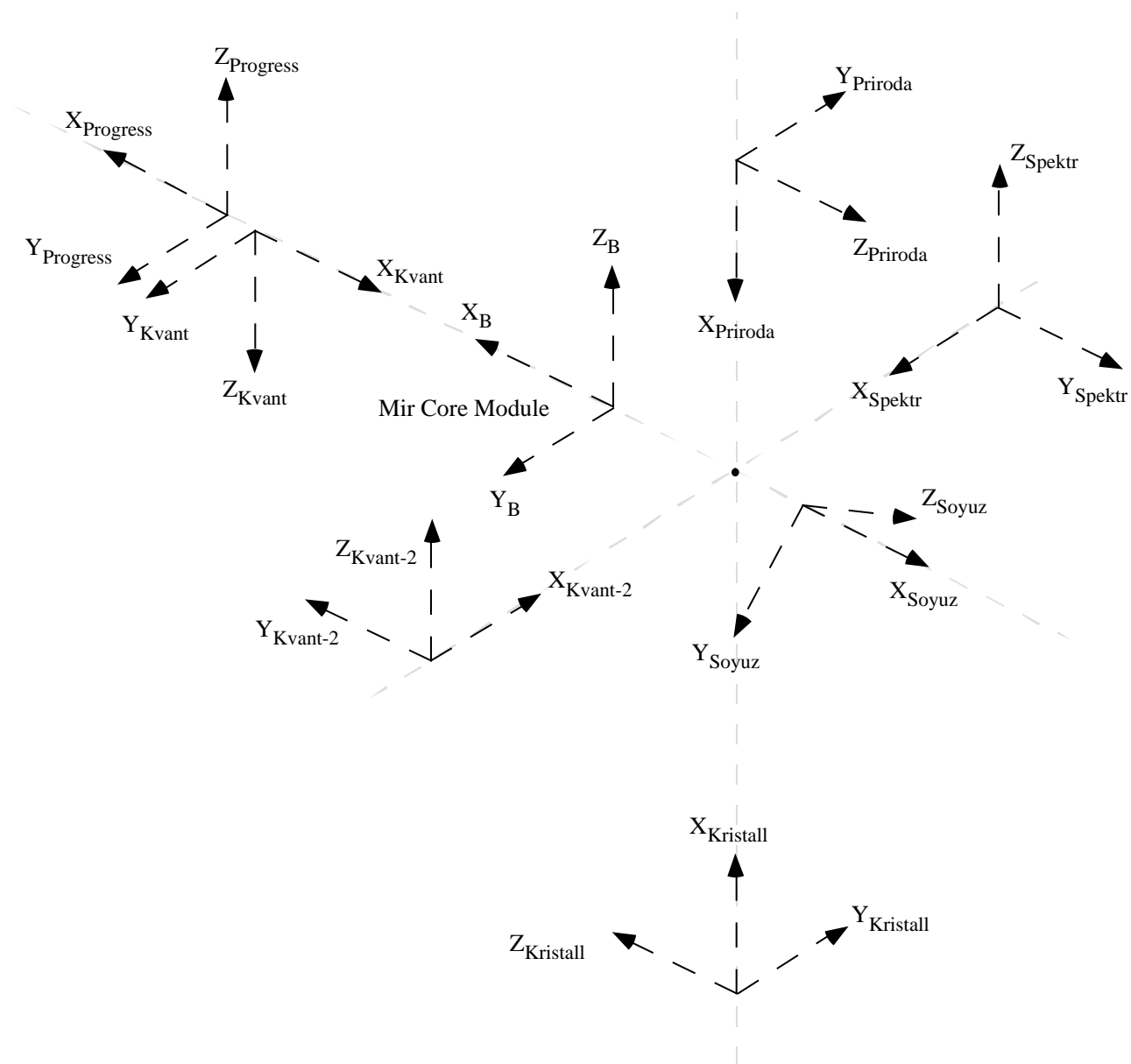


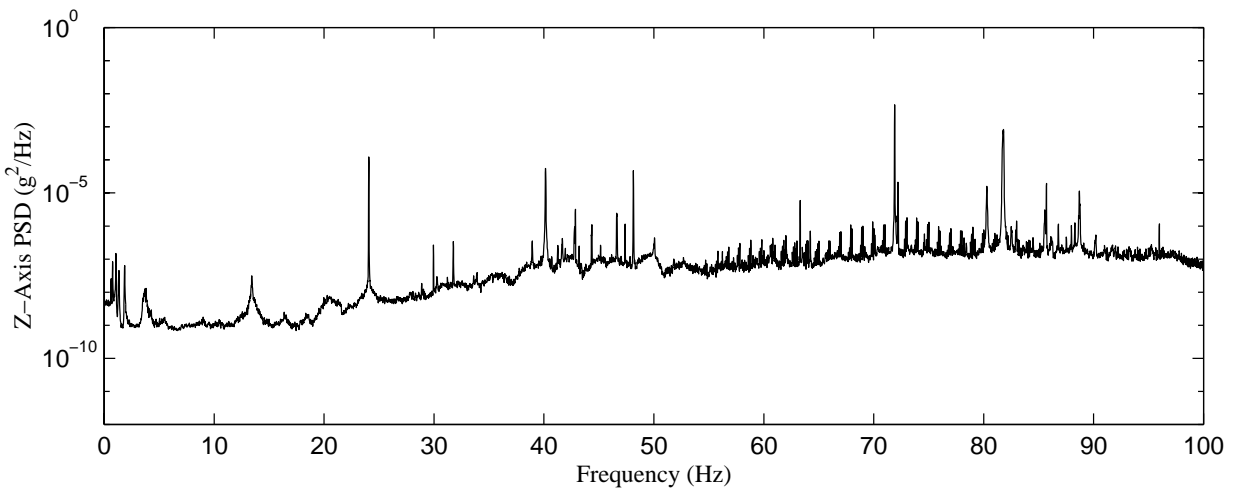
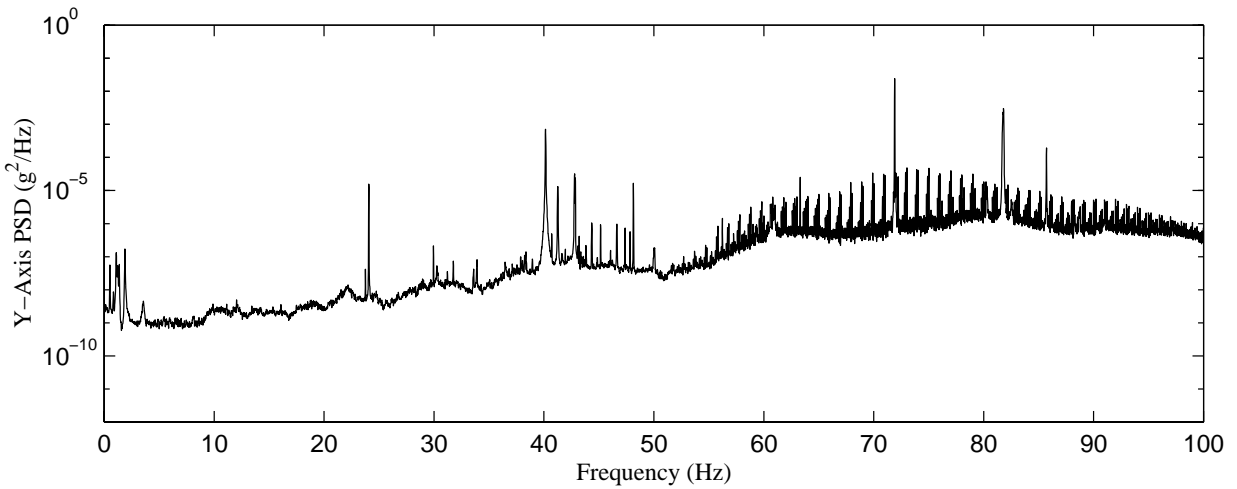
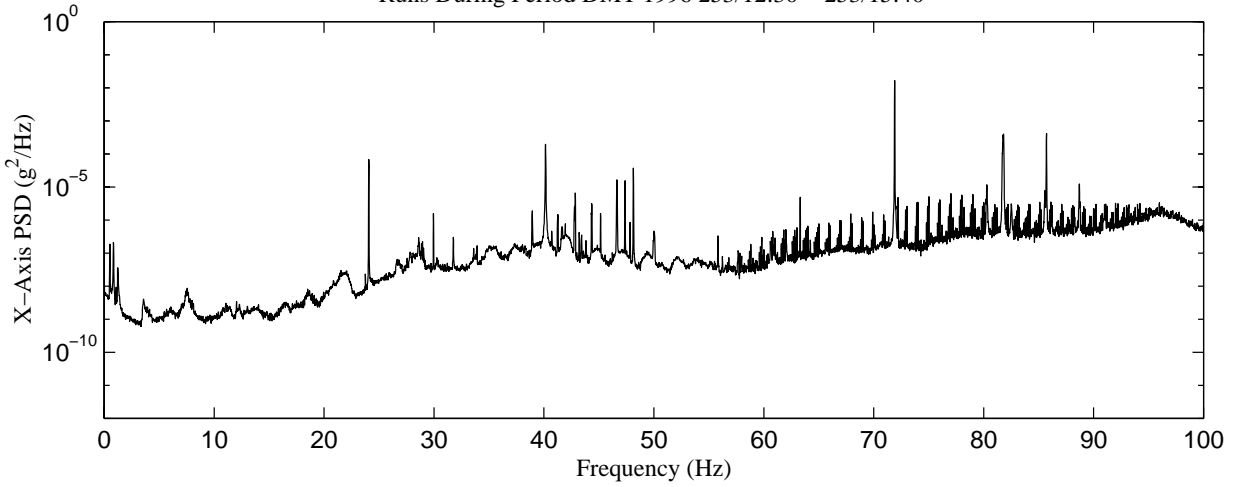
Figure 2. Mir module orientations.

Head A, 100 Hz  
fs= 500 samples per second  
dF= 0.015259 Hz

MIM Verification

MIR-1996  
SAMS TSH Coordinates

Runs During Period DMT 1996 253/12:30 – 253/15:40



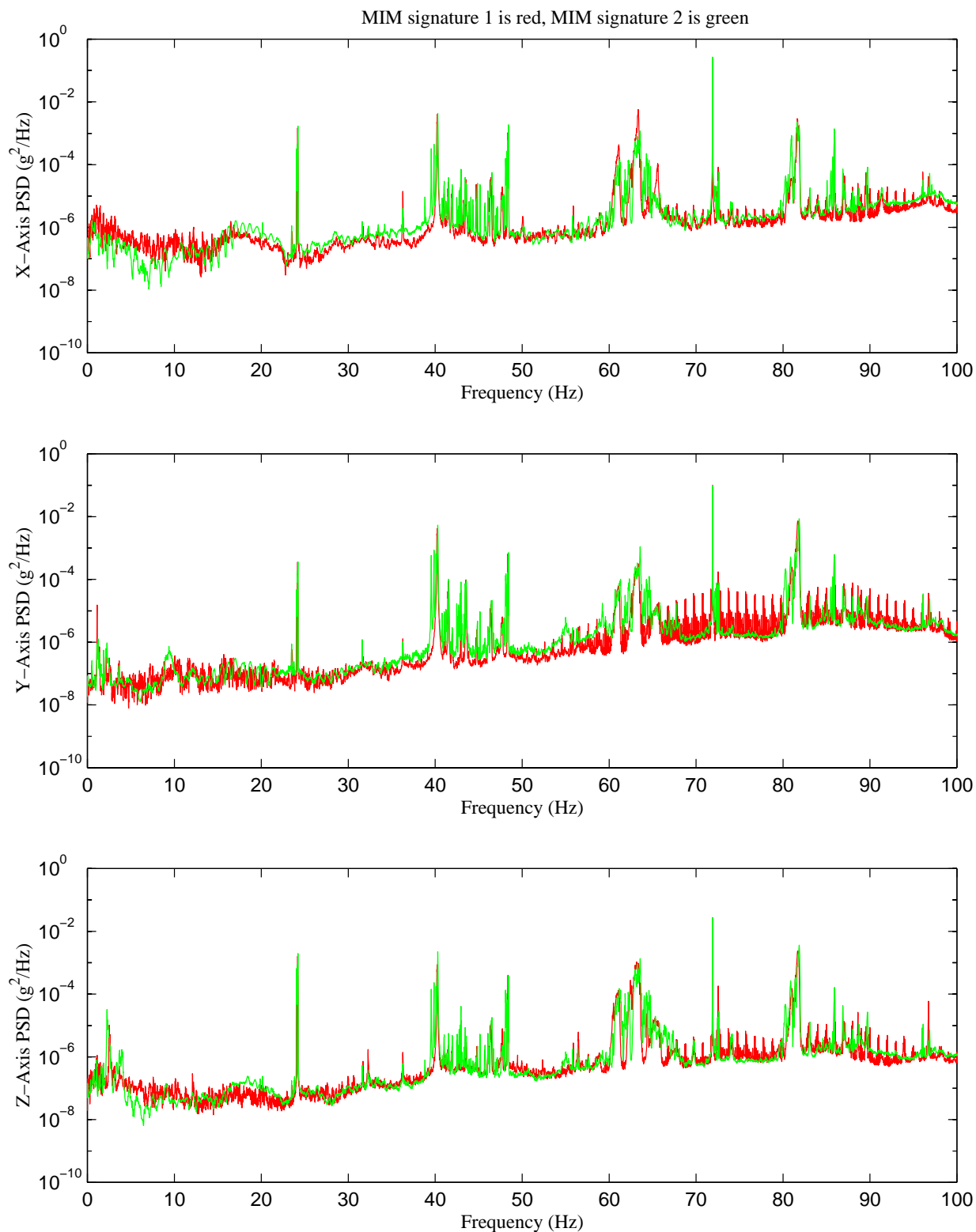
MATLAB: 24-Apr-1997, 08:27 am

Figure 3. Compilation of PSDs of SAMS data acquired during MIM verification tests.

Head A, 100 Hz  
fs= 500 samples per second  
dF= 0.015259 Hz

QUELD

MIR-1996  
TSH Coordinates



MATLAB: 21-Apr-1997, 11:08 am

Figure 4. Compilation of PSDs of SAMS data acquired during QUELD experiments, with and without the use of MIM.

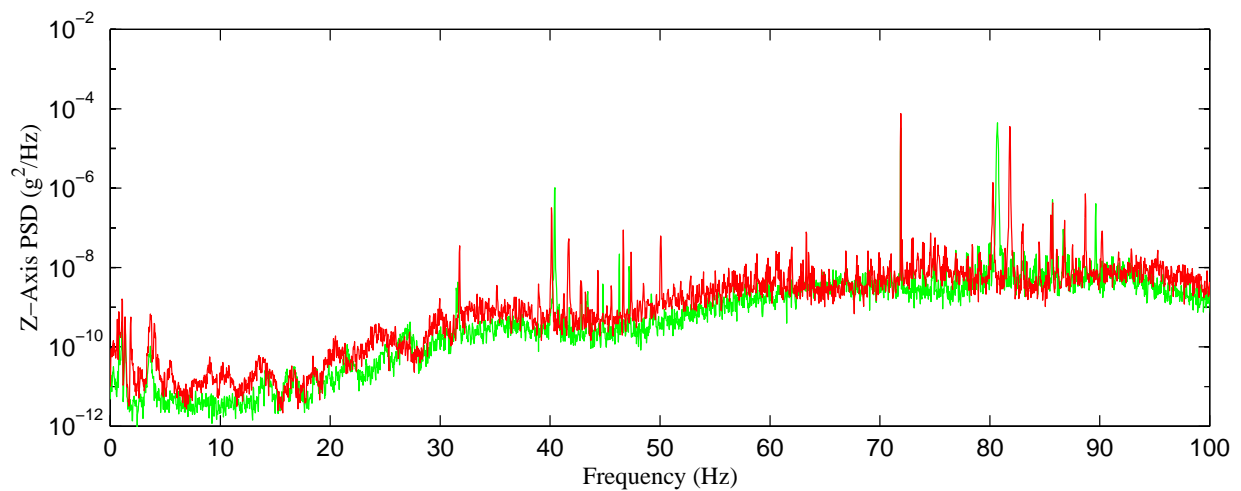
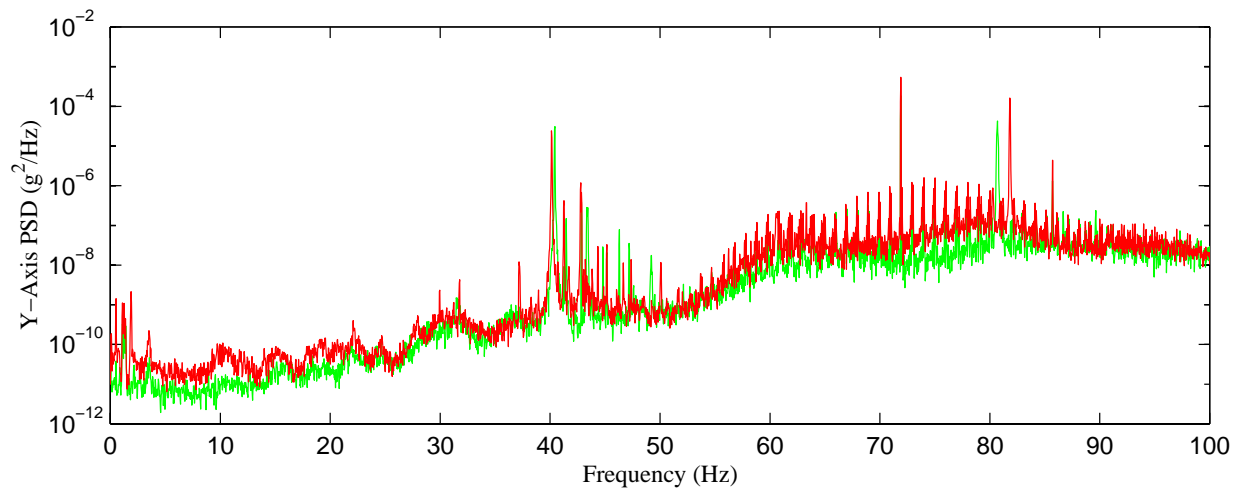
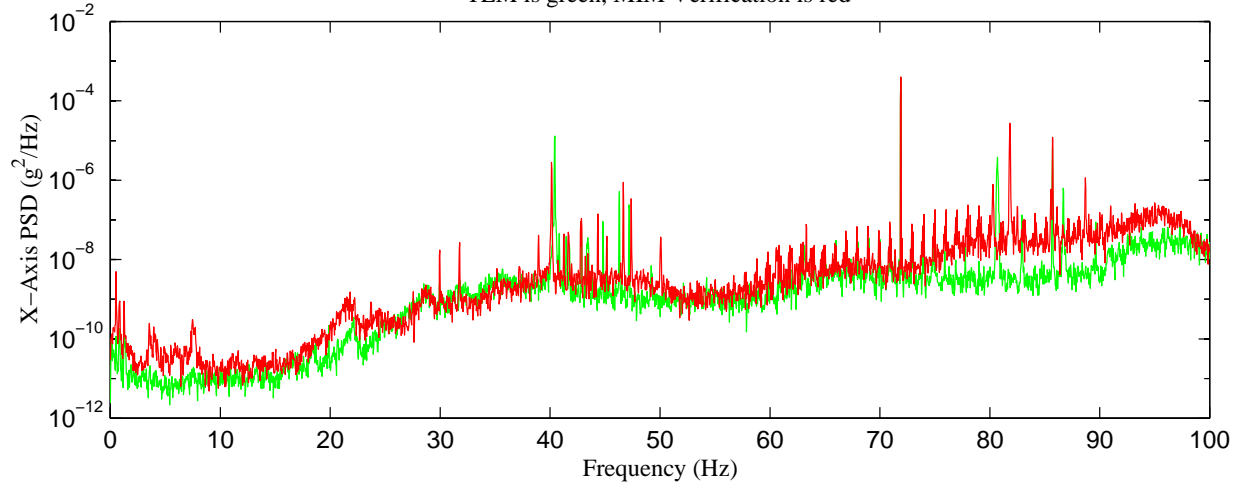


Head A, 100.0 Hz  
fs= 500.0 samples per second  
dF= 0.030518 Hz

# Comparison of TEM and MIM Verification

MIR-1996  
SAMS Coordinates  
T= 4.369 min

TEM is green, MIM Verification is red



MATLAB: 30-Apr-1997, 12:29 pm

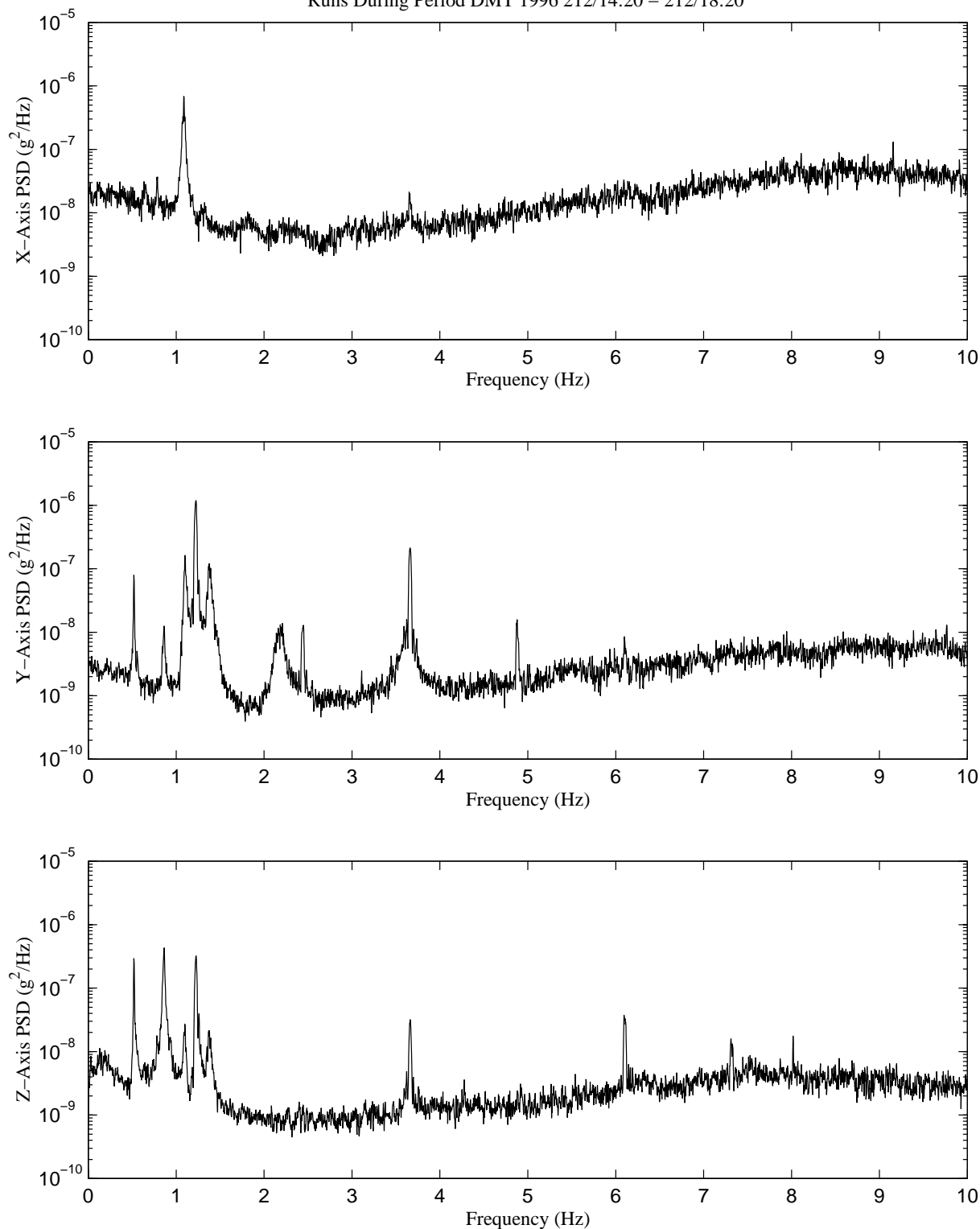
Figure 5. Compilation of PSDs of SAMS data comparing TEM and MIM verification tests of SAMS data.

Head B, 10 Hz  
fs= 50 samples per second  
dF= 0.0030518 Hz

FFFT

MIR-1996  
SAMS Coordinates

Runs During Period DMT 1996 212/14:20 – 212/18:20



MATLAB: 01-May-1997, 02:50 pm

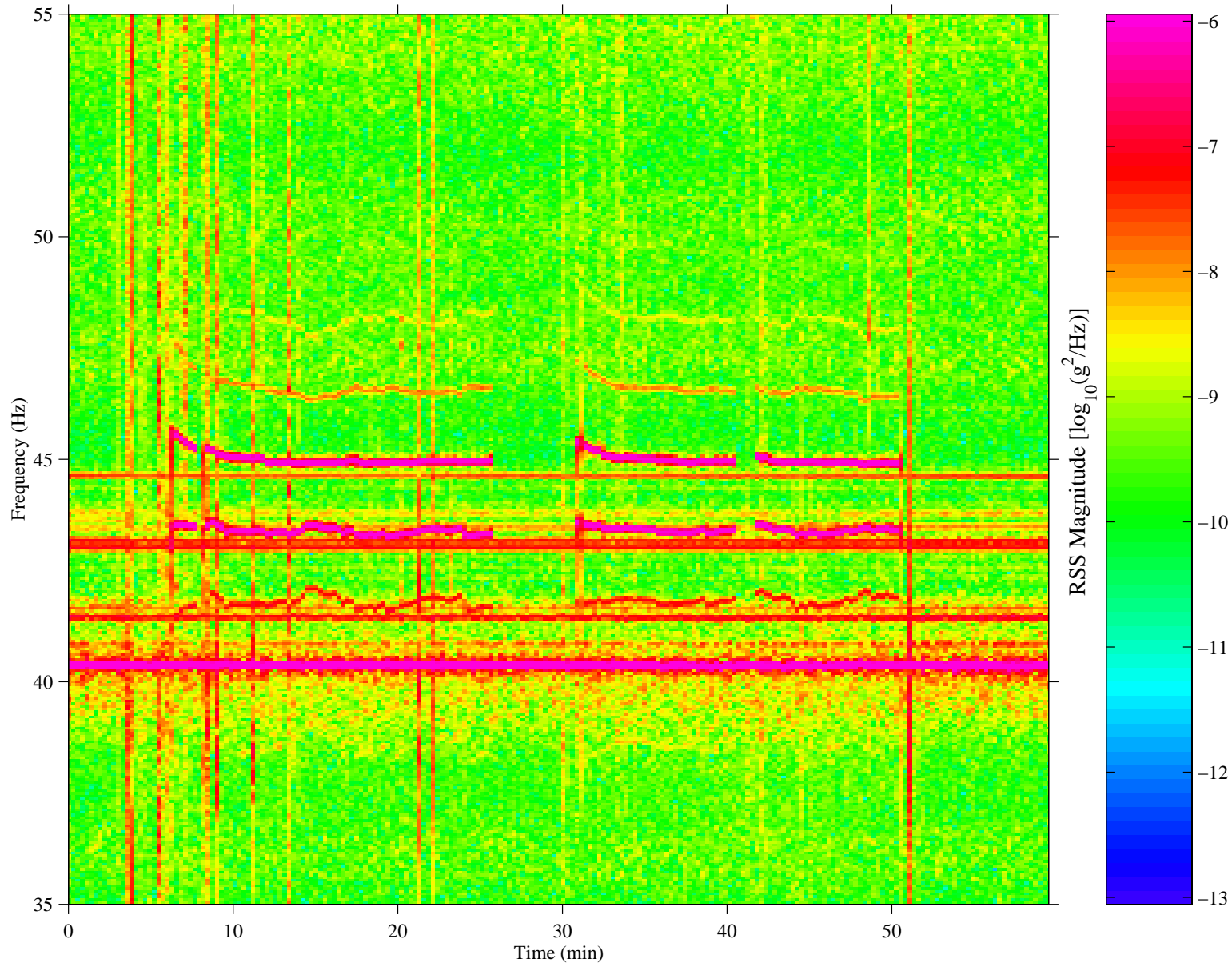
Figure 6. Compilation of PSDs of SAMS data acquired during FFFT experiments.

Head A, 100.0 Hz  
 fs= 500.0 samples per second  
 dF= 0.0610 Hz  
 dT= 0.2731 min

DMT Start at 212/19:00:00.225, Hanning k= 219

FFFT

MIR-1996  
 SAMS Coordinates



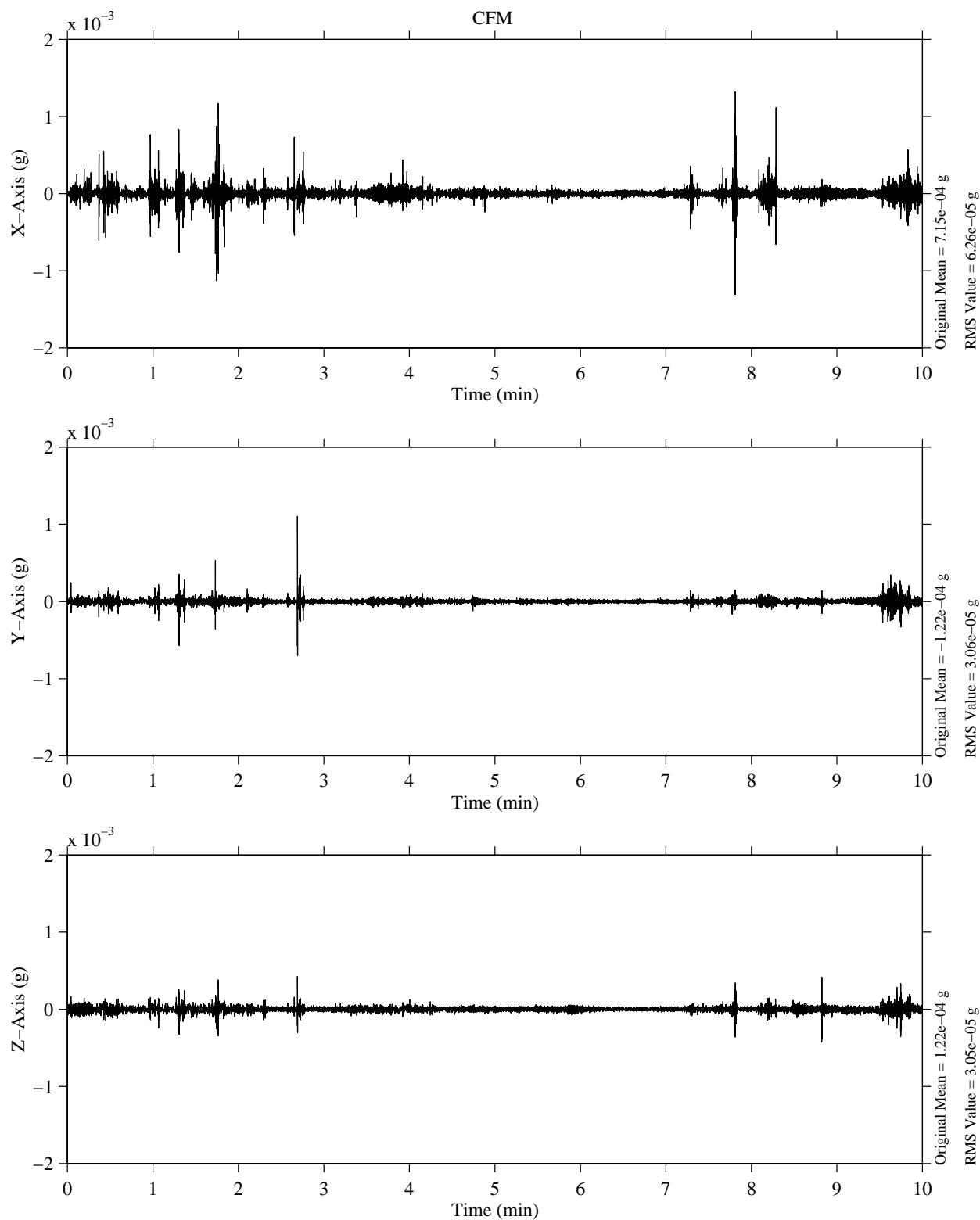
MATLAB: 22-Apr-1997, 10:55 am

Figure 7. Spectrogram of SAMS data acquired during an FFFT experiment.

Head B, 10.0 Hz  
fs= 50.0 samples per second

DMT Start at 205/15:30:00.161

MIR-1996  
SAMS Coordinates



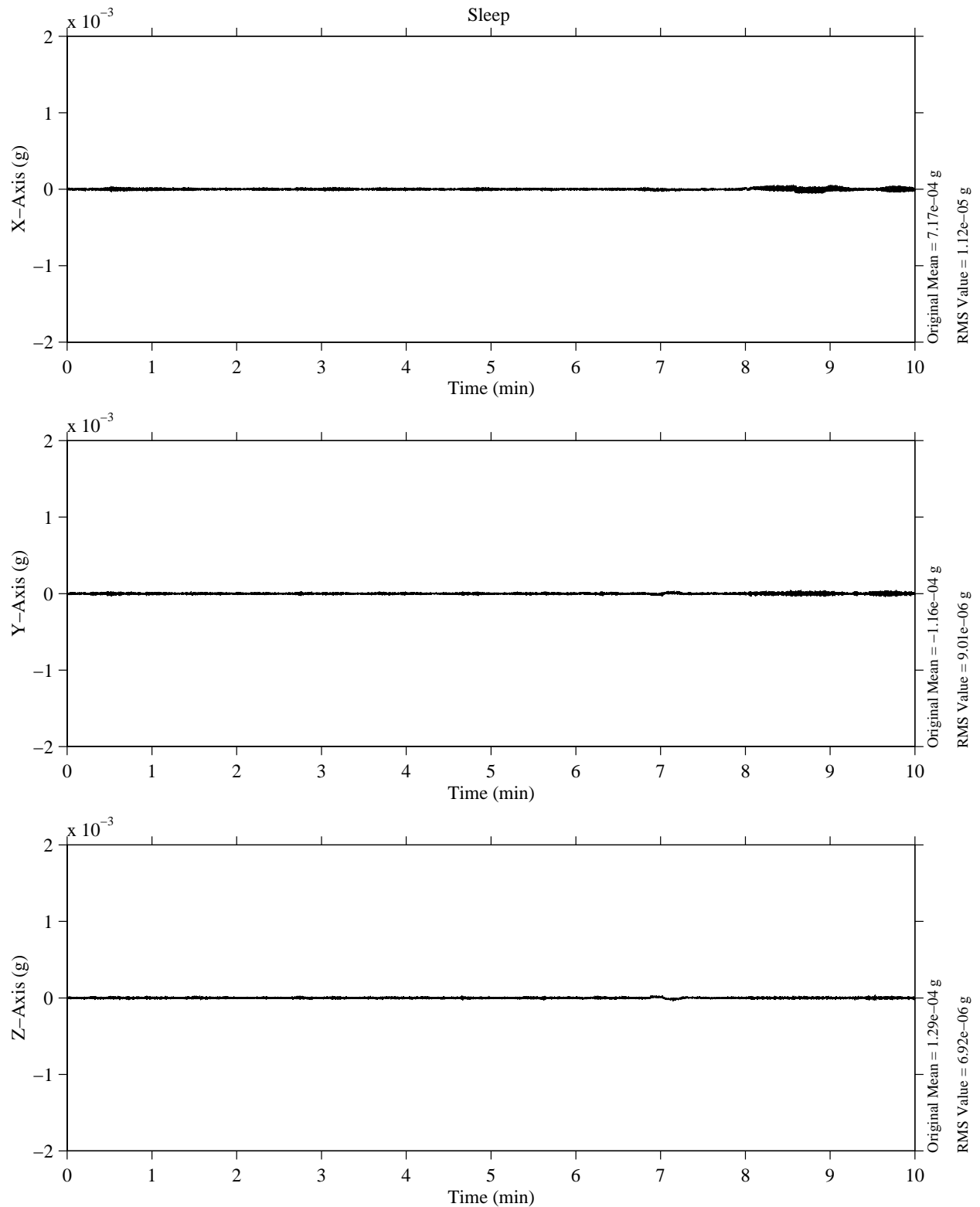
MATLAB: 05-May-1997, 10:26 am

Figure 8. Time history of SAMS data acquired during a CFM experiment.

Head B, 10.0 Hz  
fs= 50.0 samples per second

DMT Start at 206/01:19:59.997

MIR-1996  
SAMS Coordinates



MATLAB: 05-May-1997, 10:40 am

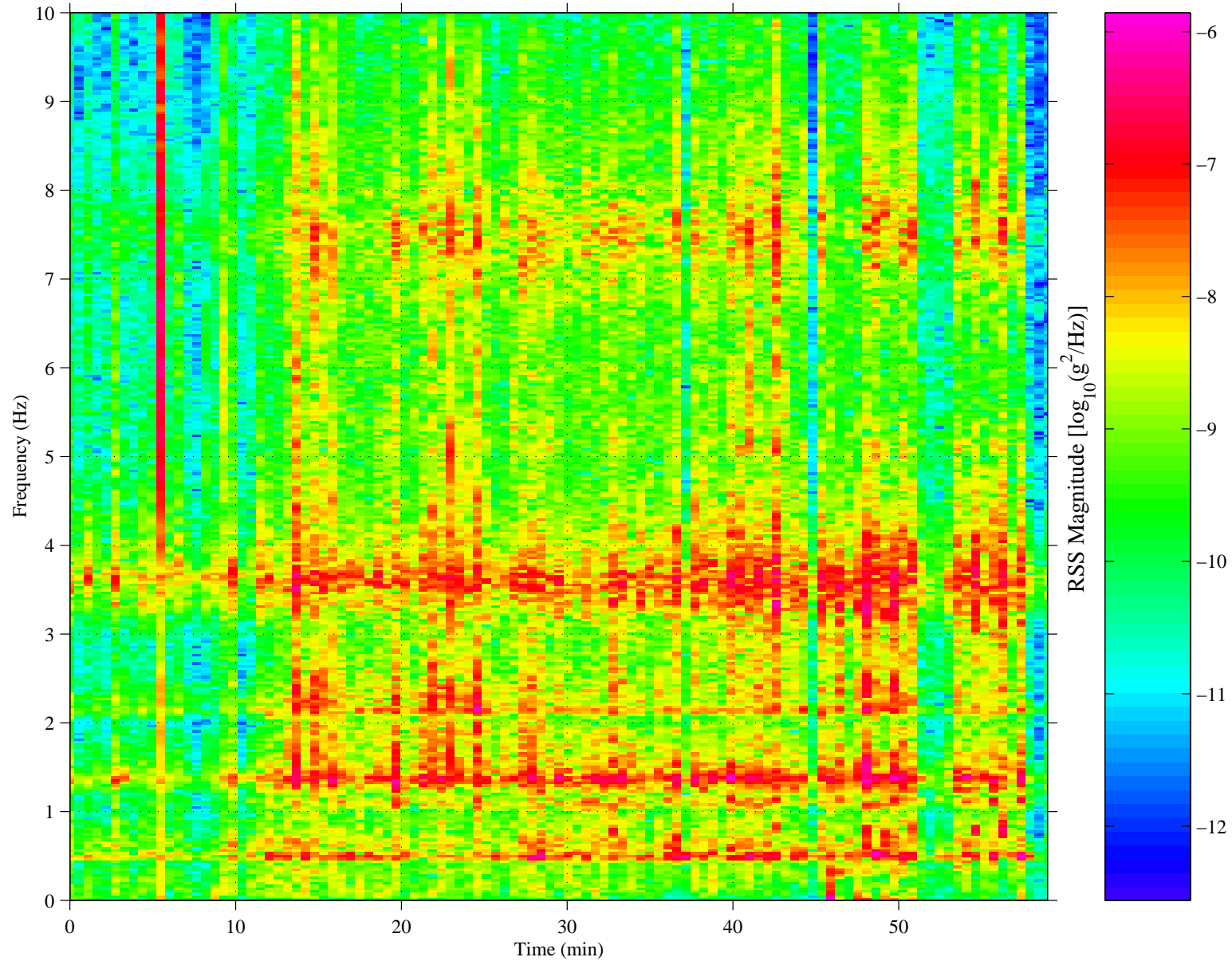
Figure 9. Time history of SAMS data acquired during a crew sleep period.

Head A, 100.0 Hz  
 fs= 500.0 samples per second  
 $\Delta F = 0.0305$  Hz  
 $\Delta T = 0.5461$  min

DMT Start at 146/02:00:00.626, Hanning k= 109

Mir Increment 2: Solar Panel Deploy

MIR-1996  
 SAMS Coordinates



MATLAB: 01-May-1997, 01:32 pm

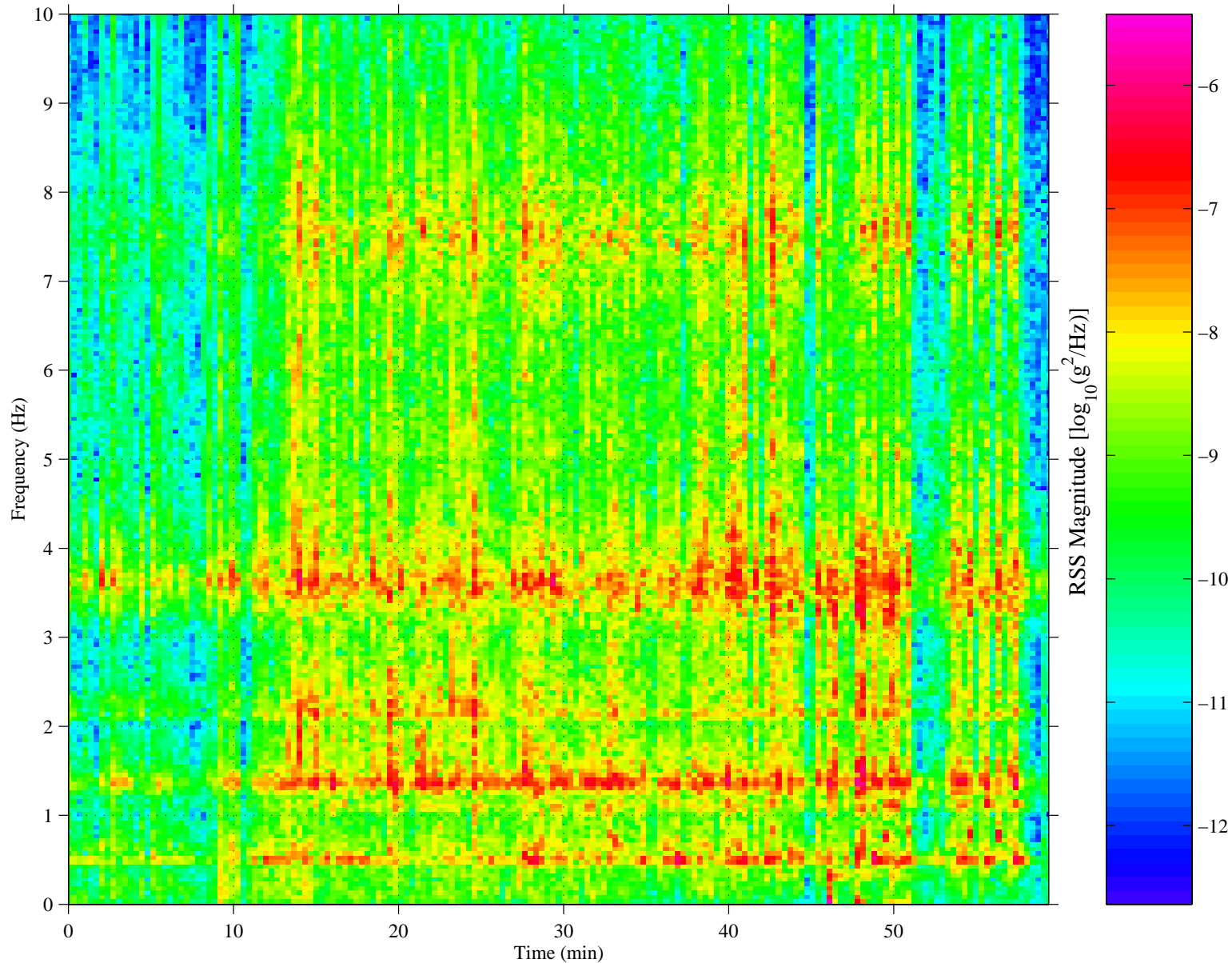
Figure 10. Spectrogram of TSH A SAMS data collected during an EVA to deploy solar panels.

Head B, 10.0 Hz  
 fs= 50.0 samples per second  
 dF= 0.0488 Hz  
 dT= 0.3413 min

DMT Start at 146/02:00:00.626, Hanning k= 175

Mir Increment 2: Solar Panel Deploy

MIR-1996  
 SAMS Coordinates



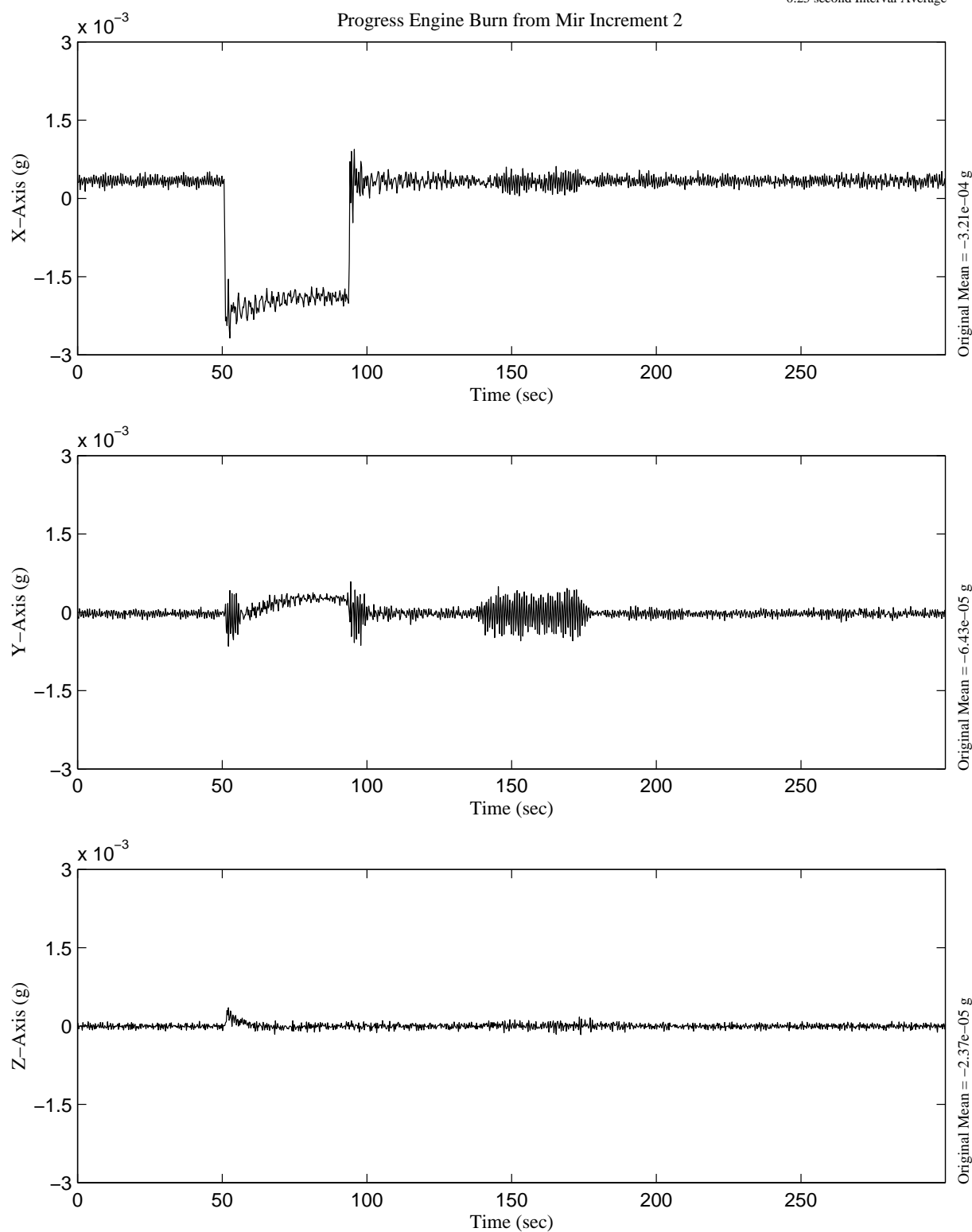
MATLAB: 01-May-1997, 01:42 pm

Figure 11. Spectrogram of TSH B SAMS data collected during an EVA to deploy solar panels.

Head A, 100.0 Hz  
fs= 500.0 samples per second

DMT Start at 184/11:44:59.998

MIR-1996  
SAMS Coordinates  
0.25 second Interval Average



MATLAB: 29-Apr-1997, 10:59 am

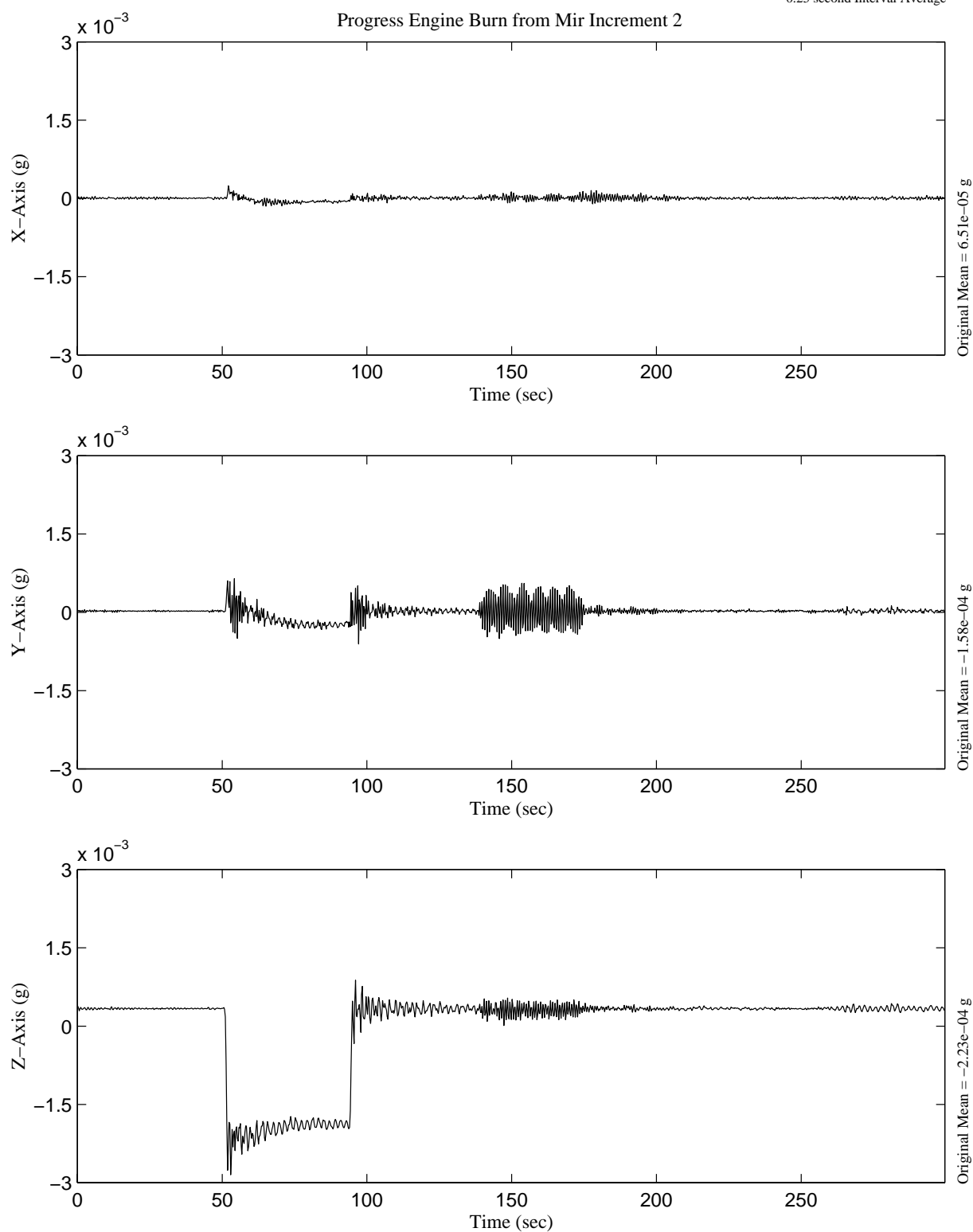
Figure 12. Time history of TSH A SAMS data showing the acceleration effects of a Progress engine burn.



Head B, 10.0 Hz  
fs= 50.0 samples per second

DMT Start at 184/11:44:59.992

MIR-1996  
SAMS Coordinates  
0.25 second Interval Average



MATLAB: 29-Apr-1997, 11:02 am

Figure 13. Time history of TSH B SAMS data showing the acceleration effects of a Progress engine burn.

Head A, 100.0 Hz

fs= 500.0 samples per second

dF= 0.030518 Hz

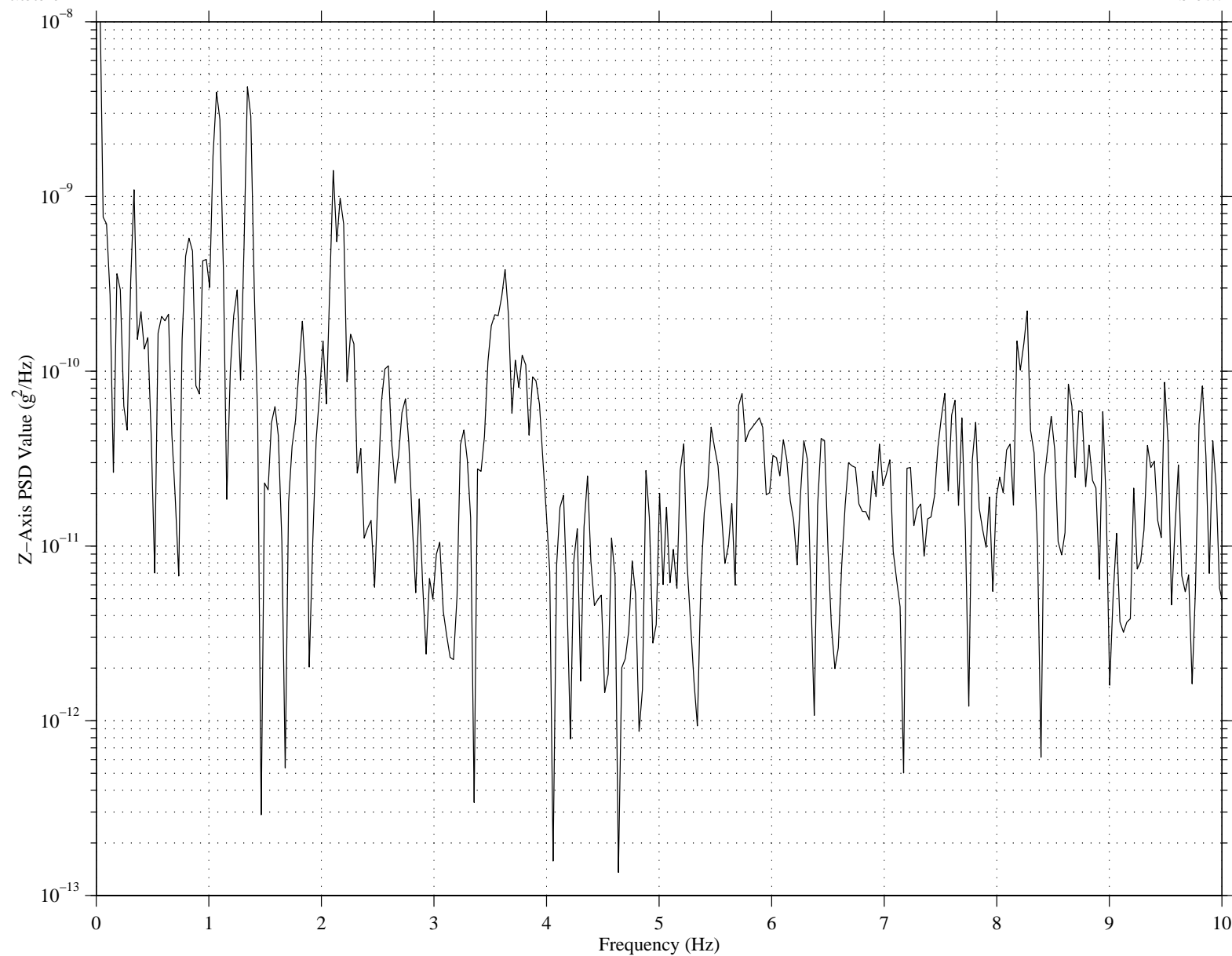
DMT Start at 184/11:45:52.248, Hanning k=1

Progress Engine Burn from Mir Increment 2

MIR-1996

SAMS Coordinates

T= 41.518 sec



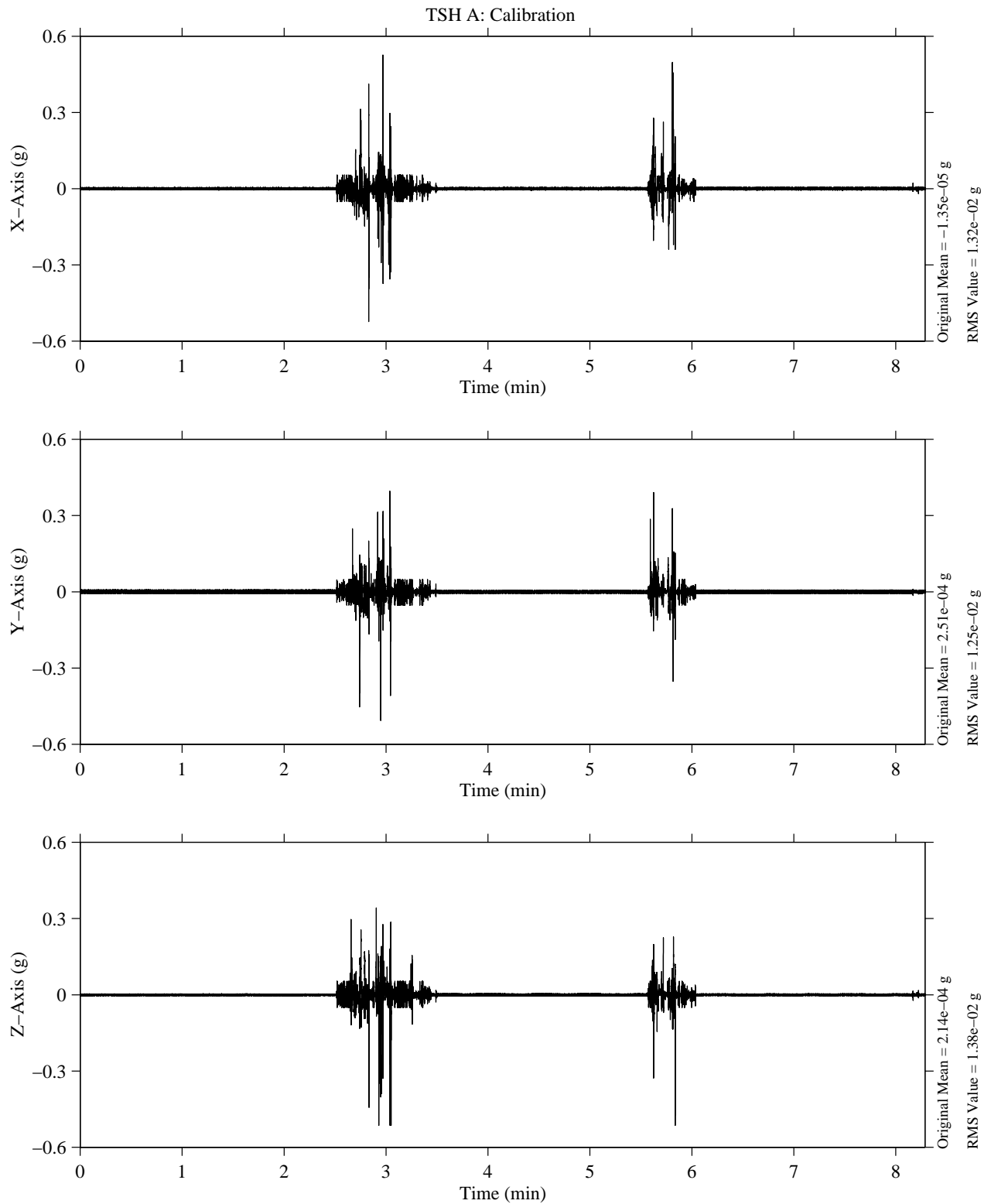
MATLAB: 29-Apr-1997, 11:18 am

Figure 14. Power Spectral Density of SAMS TSH A data collected during the Progress engine burn event.

Head A, 100.0 Hz  
fs= 500.0 samples per second

DMT Start at 169/14:47:17.402

MIR-1996  
SAMS Coordinates



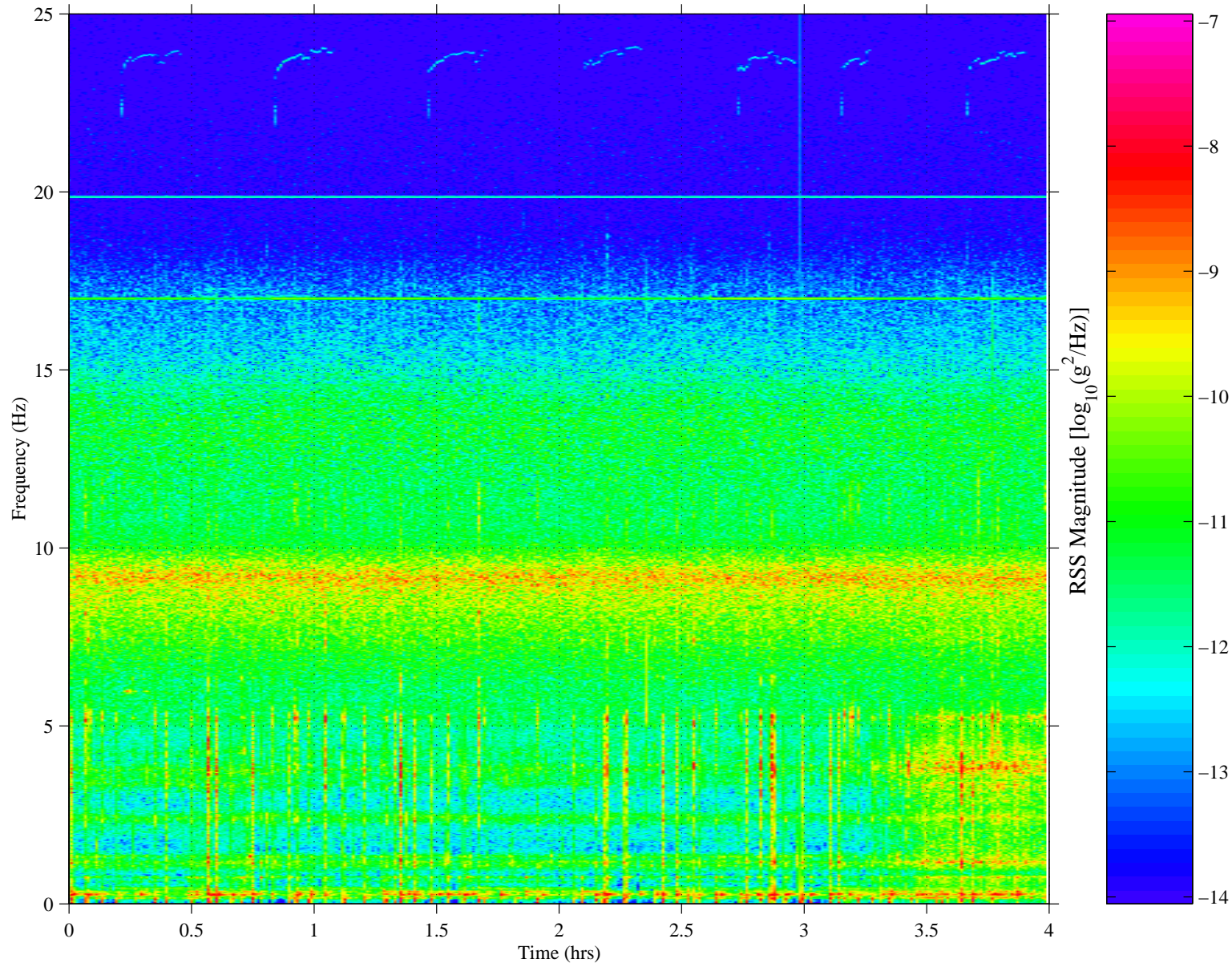
MATLAB: 07-May-1997, 09:53 am

Figure 15. Time history of SAMS TSH A data showing an on-orbit SAMS calibration activity.

Head B, 10.0 Hz  
 fs= 50.0 samples per second  
 dF= 0.0244 Hz  
 dT= 40.9836 sec

DMT Start at 084/20:00:00.519, Hanning k= 351  
 Mir Increment 2 TSH-B: Mir/Atlantis (STS-76) Docked

MIR-1996  
 SAMS Coordinates



MATLAB: 30-Apr-1997, 08:49 am

Figure 16. Spectrogram of TSH B SAMS data showing the microgravity environment of the Mir/Atlantis (STS-76) complex.

Head A, 100.0 Hz

fs= 500.0 samples per second

dF= 0.03052 Hz

DMT Start at 125/09:00:00.691, Boxcar k=18  
SAMS data from Mir (year 1996): 24 Hz Compressor

MIR-1996

SAMS Coordinates

T= 9.988 min

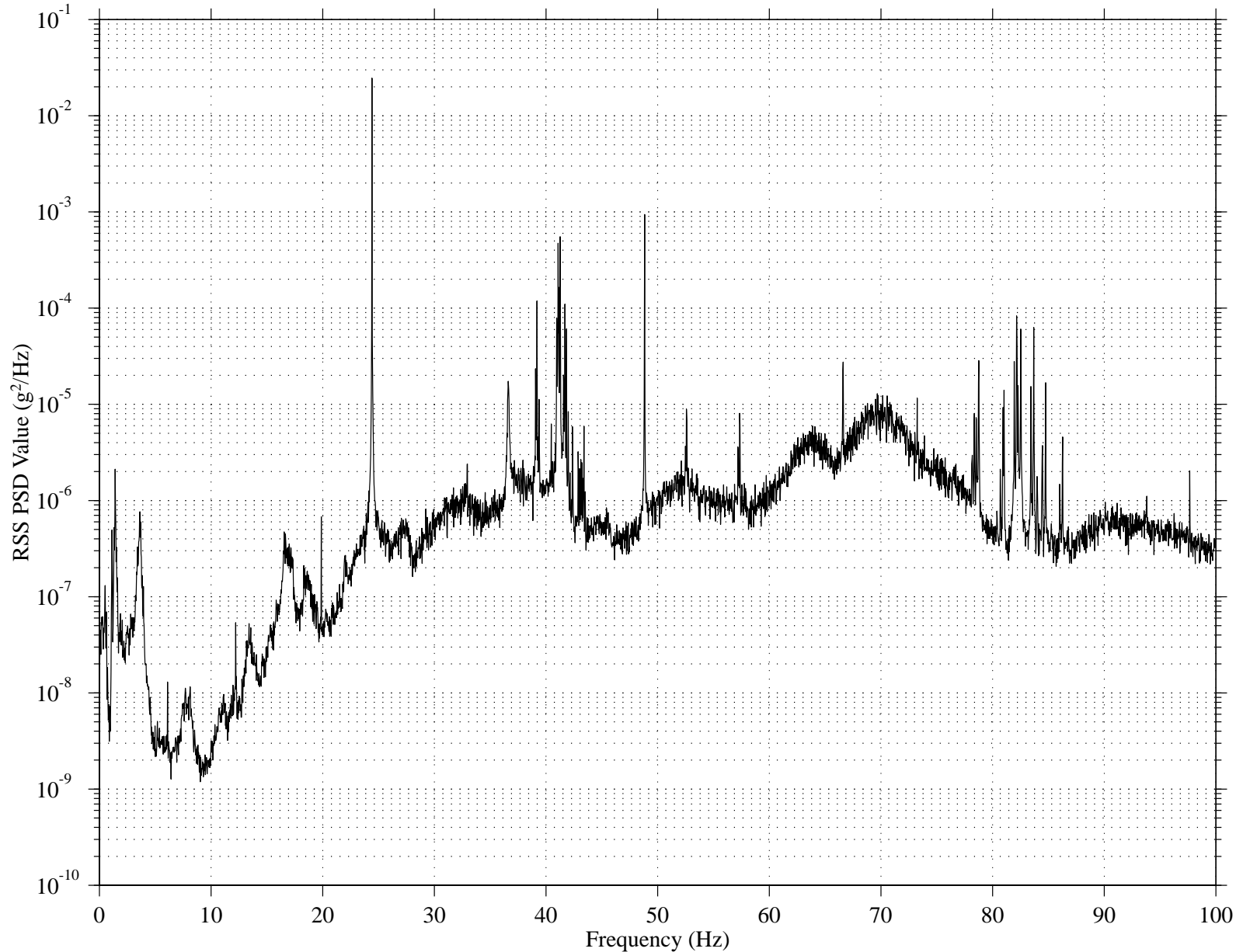


Figure 17. Power Spectral Density of SAMS TSH A data showing BKV-3 frequencies.

MATLAB: 11-Feb-97, 9:14 am



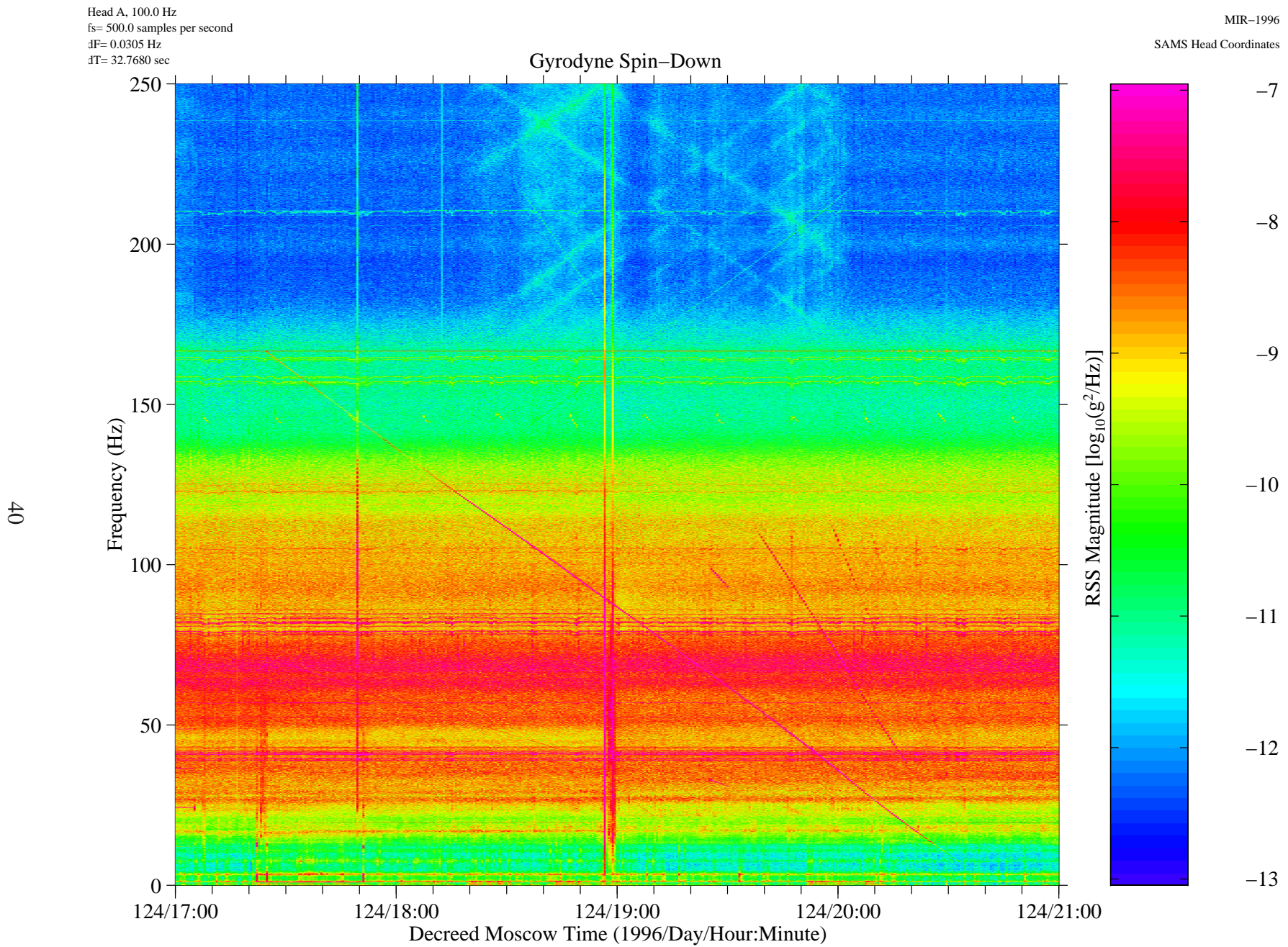


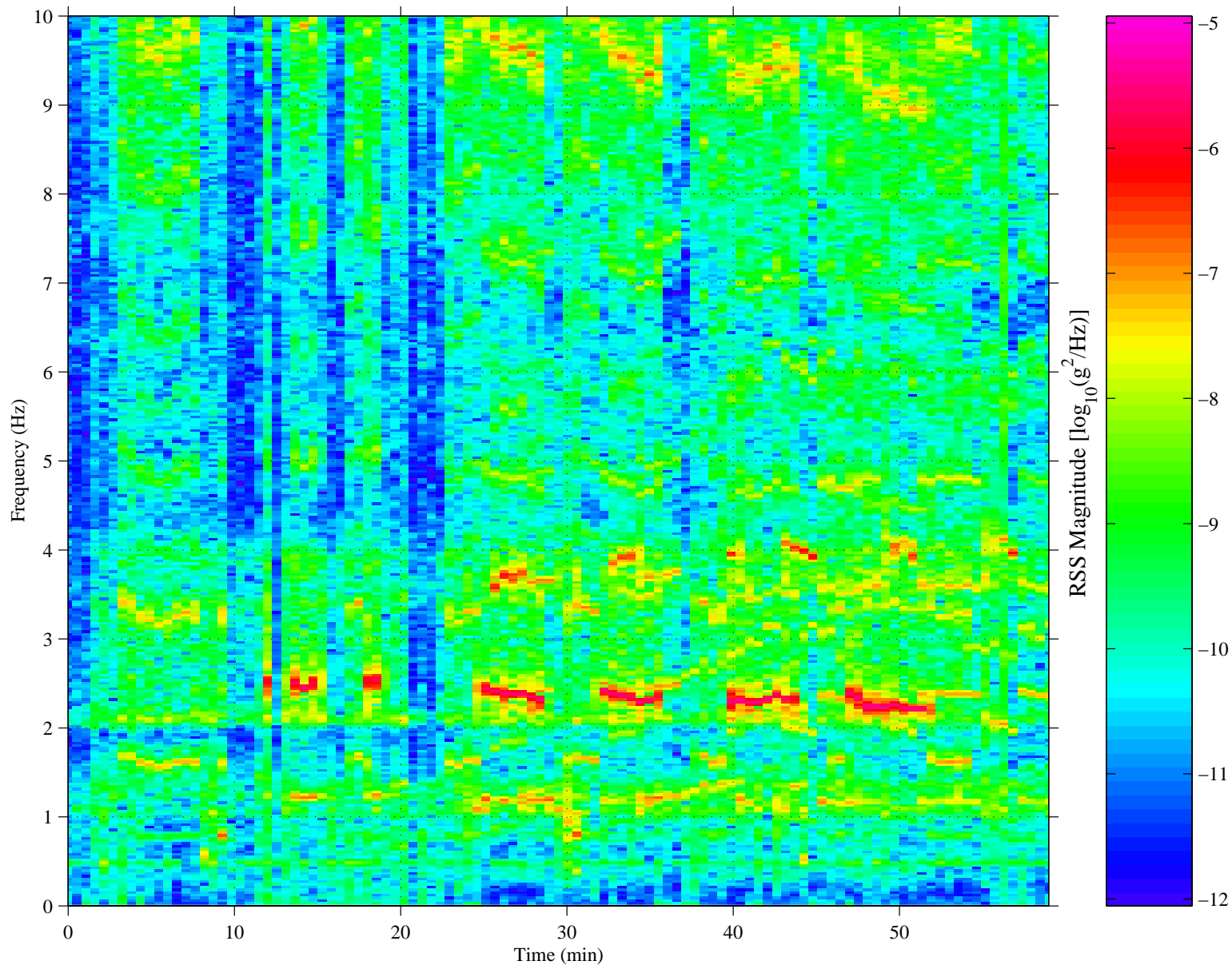
Figure 18. Spectrogram of TSH A data showing a gyrodyne spin-down activity.

Head A, 100.0 Hz  
 fs= 500.0 samples per second  
 dF= 0.0305 Hz  
 dT= 0.5461 min

DMT Start at 180/18:40:00.673, Hanning k= 109

SAMS TSH A: Exercise on Mir

MIR-1996  
 SAMS Coordinates



MATLAB: 07-May-1997, 01:20 pm

Figure 19. Spectrograms of SAMS TSH A data collected during a crew exercise period

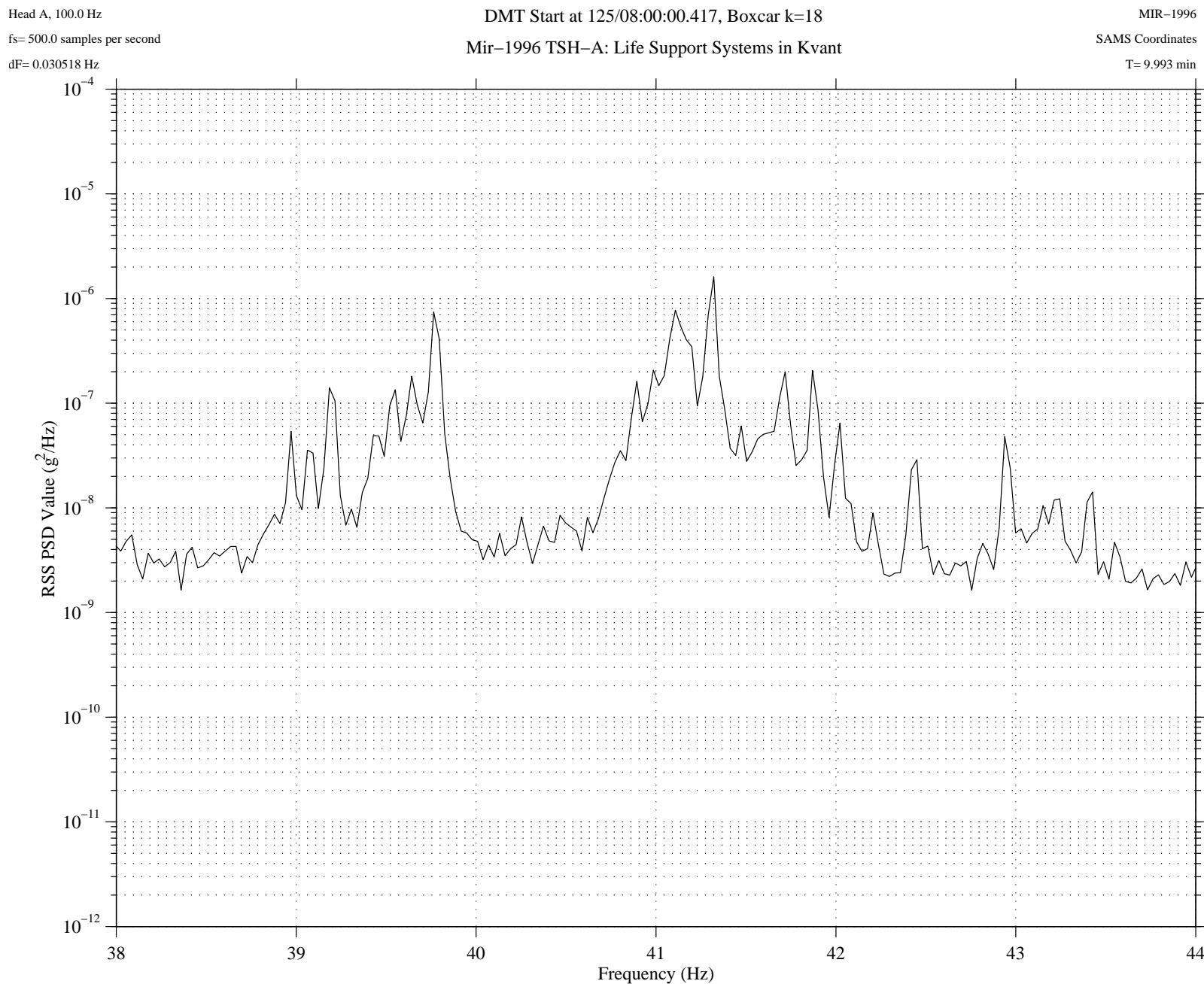


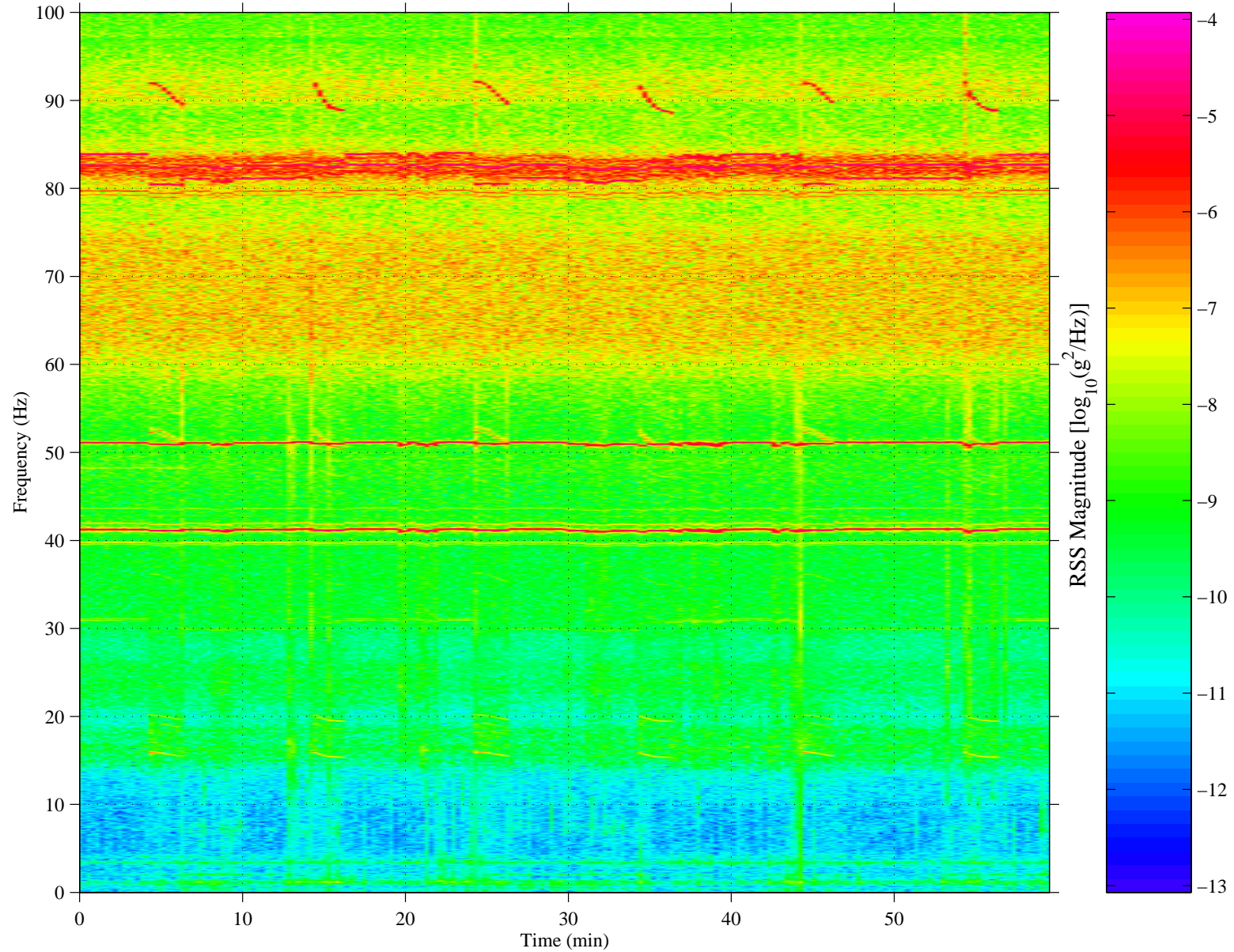
Figure 20. Power Spectral Density of SAMS TSH A data showing frequencies related to the life-support systems in the Kvant module.



Head A, 100.0 Hz  
fs= 500.0 samples per second  
dF= 0.0610 Hz  
dT= 0.2731 min

DMT Start at 216/20:00:00.166, Hanning k= 219  
Mir year 1995: Life Support Systems in Kvant

MIR-1995  
SAMS Coordinates



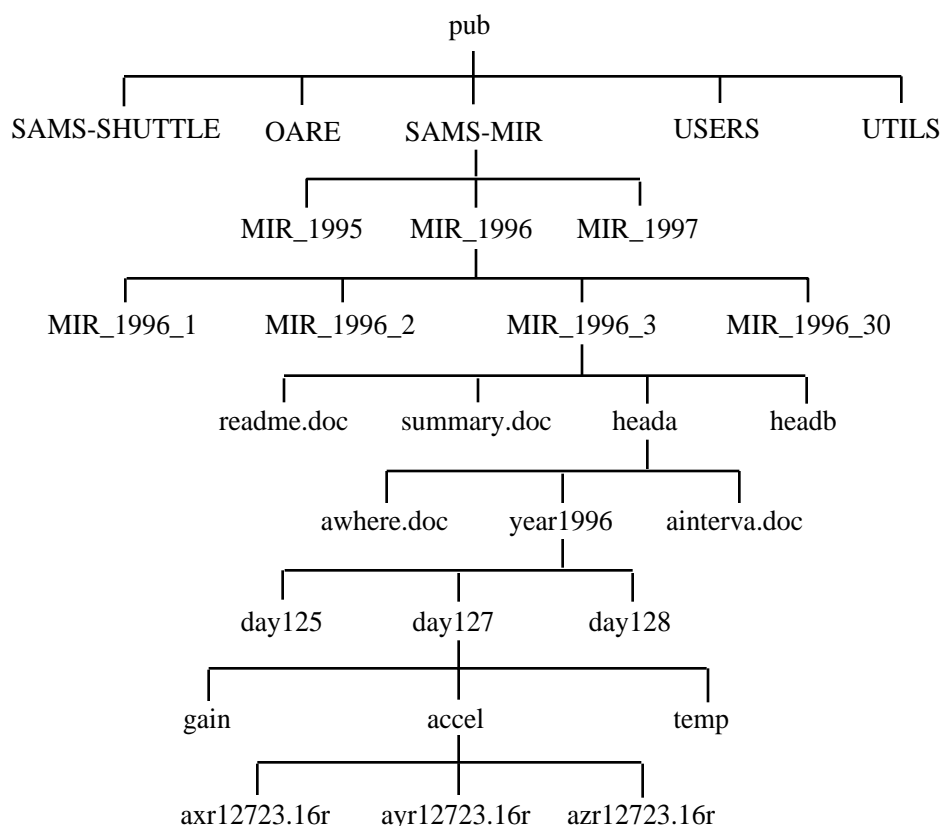
MATLAB: 07-May-1997, 12:38 pm

Figure 21. Spectrogram of SAMS TSH A showing frequencies related to life-support systems in the Kvant module.

## Appendix A: Accessing Acceleration Data via the Internet

SAMS and OARE data are available over the internet from the NASA LeRC file server “beech.lerc.nasa.gov”. Previously, SAMS data were made available on CD-ROM, but distribution of data from current (and future) missions will be primarily through this internet file server.

SAMS data files are arranged in a standard tree-like structure. Data are first separated based upon mission. Then, data are further subdivided based upon some portion of the mission, head, year (if applicable), day, and finally type of data file (acceleration, temperature, or gain). Effective November 1, 1996, there has been a minor reorganization of the beech.lerc.nasa.gov file server. There are now two locations for SAMS data: a directory called SAMS-SHUTTLE and a directory called SAMS-MIR. Under the SAMS-SHUTTLE directory, the data are segregated by mission. Under the SAMS-MIR directory, the data are segregated by year. The following figure illustrates this structure.



The SAMS data files (located at the bottom of the tree structure) are named based upon the contents of the file. For example, a file named “axm00102.15r” would contain head A data for the x-axis for day 001, hour 02, file 1 of 5. The readme.doc files give a complete explanation of the file naming convention.

Data access tools for different computer platforms (MS-DOS, Macintosh, SunOS, and MS-Windows) are available in the /pub/UTILS directory.

The NASA LeRC beech file server can be accessed via anonymous File Transfer Protocol (ftp), as follows:

- 1) Open an ftp connection to "beech.lerc.nasa.gov"
- 2) Login as userid "anonymous"
- 3) Enter your e-mail address as the password
- 4) Change directory to pub
- 5) List the files and directories in the pub directory
- 6) Change directories to the area of interest
- 7) Change directories to the mission of interest
- 8) Enable binary file transfers
- 9) Use the data file structures (described above) to locate the desired files
- 10) Transfer the desired files

If you encounter difficulty in accessing the data using the file server, please send an electronic mail message to "pims@lerc.nasa.gov". Please describe the nature of the difficulty and also give a description of the hardware and software you are using to access the file server. If you are interested in requesting specific data analysis or information from the PIMS team, also send e-mail to pims@lerc.nasa.gov or call the PIMS Project Manager, Duc Truong at (216) 433-8394.

## Appendix B: SAMS Color Spectrograms TSH A

The Principal Investigator Microgravity Services (PIMS) group has further processed SAMS data to produce the plots shown here. PSD magnitude versus frequency versus time (spectrogram) plots are shown here with up to 6 hours worth of data per page.

Color spectrograms are used to show how the microgravity environment varies in intensity with respect to both the time and frequency domains. These spectrograms are provided as an overview of the frequency characteristics of the SAMS data. Each spectrogram is a composite of 6 hour's worth of data. The time resolution used to compute the spectrograms seen here is 16.384 seconds. This corresponds to a frequency resolution of 0.0610 Hz.

These data were collected at 500 samples per second, and a 100 Hz low pass filter was applied to the data by the SAMS unit prior to digitization. Prior to plot production, the raw SAMS data were compensated for gain changes, and then demeaned. Demeaning was accomplished by analyzing individual sections with a nominal length of 12 minutes. Users who are interested in further details for either of these operations are encouraged to contact the PIMS group.

### Power Spectral Density versus Frequency versus Time Calculations

In order to produce the spectrogram image, Power Spectral Densities were computed for successive time intervals (the length of the interval is equal to the time resolution). For the PSD computation, a Hanning window was applied. In order to combine all three axes into a single plot to show an overall level, a Vector-Magnitude (VM) operation was performed. Stated mathematically:

$$VM_k = \sqrt{PSD_{x_k}^2 + PSD_{y_k}^2 + PSD_{z_k}^2}.$$

By imaging the base 10 logarithm ( $\log_{10}$ ) magnitude as a color and stacking successive PSDs from left to right, variations of acceleration magnitude and frequency are shown as a function of time. Colors are assigned to discrete magnitude ranges, so that there are 64 colors assigned to the entire range of magnitudes shown.

The colorbar limits are chosen in order to maximize the data value and visibility in a given set of spectrogram plots. Data which fall outside of these limits will be imaged as either the highest or lowest magnitude, depending on which side they have saturated. For this report, less than 1% of the total points

lie below the lower limit, and less than 1% of the total points lie above the upper limit. If an area of interest seems to be saturated, care should be taken in that the actual values may lie above or below the color mapping shown on the plot.

Due to the nature of spectrograms, care should be taken to not merely read a color's numeric value as being the "amount" of acceleration that is present at a given frequency. In order to get this type of information, the PSDs must be integrated between two frequencies. These frequencies (lower and upper) form the "band" of interest. The result of this integration is the  $g_{\text{RMS}}$  acceleration level in the  $[f_{\text{lower}}, f_{\text{upper}}]$  band. The PIMS group is able to provide this type of analysis on a per-request basis.

Plot gaps (if any exist) are shown by either white or dark blue areas on the page. Care should be taken to not mistake a plot gap (represented by a blue vertical band) with a quiet period. If a plot gap exists for an entire plot (or series of successive plots), a comment is placed on the page to let the user know there is a gap in the data. These "no data available" comments will not show exact times for which the data are not available, but will only indicate missing plots.

#### Contacting PIMS

To request additional analysis or information, users are encouraged to send an e-mail to [pims@lerc.nasa.gov](mailto:pims@lerc.nasa.gov), or FAX a request to (216) 433-8660.

## Appendix C: SAMS Color Spectrograms for TSH B

The Principal Investigator Microgravity Services (PIMS) group has further processed SAMS data to produce the plots shown here. PSD magnitude versus frequency versus time (spectrogram) plots are shown here with up to 6 hours worth of data per page.

Color spectrograms are used to show how the microgravity environment varies in intensity with respect to both the time and frequency domains. These spectrograms are provided as an overview of the frequency characteristics of the SAMS data. Each spectrogram is a composite of 6 hour's worth of data. The time resolution used to compute the spectrograms seen here is 65.536 seconds. This corresponds to a frequency resolution of 0.0153 Hz.

These data were collected at 50 samples per second, and a 10 Hz low pass filter was applied to the data by the SAMS unit prior to digitization. Prior to plot production, the raw SAMS data were compensated for gain changes, and then demeaned. Demeaning was accomplished by analyzing individual sections with a nominal length of 60 minutes. Users who are interested in further details for either of these operations are encouraged to contact the PIMS group.

### Power Spectral Density versus Frequency versus Time Calculations

In order to produce the spectrogram image, Power Spectral Densities were computed for successive time intervals (the length of the interval is equal to the time resolution). For the PSD computation, a Hanning window was applied. In order to combine all three axes into a single plot to show an overall level, a Vector-Magnitude (VM) operation was performed. Stated mathematically:

$$VM_k = \sqrt{PSD_{x_k}^2 + PSD_{y_k}^2 + PSD_{z_k}^2}.$$

By imaging the base 10 logarithm ( $\log_{10}$ ) magnitude as a color and stacking successive PSDs from left to right, variations of acceleration magnitude and frequency are shown as a function of time. Colors are assigned to discrete magnitude ranges, so that there are 64 colors assigned to the entire range of magnitudes shown.

The colorbar limits are chosen in order to maximize the data value and visibility in a given set of spectrogram plots. Data which fall outside of these limits will be imaged as either the highest or lowest magnitude, depending on which side they have saturated. For this report, less than 1% of the total points

lie below the lower limit, and less than 1% of the total points lie above the upper limit. If an area of interest seems to be saturated, care should be taken in that the actual values may lie above or below the color mapping shown on the plot.

Due to the nature of spectrograms, care should be taken to not merely read a color's numeric value as being the "amount" of acceleration that is present at a given frequency. In order to get this type of information, the PSDs must be integrated between two frequencies. These frequencies (lower and upper) form the "band" of interest. The result of this integration is the  $g_{\text{RMS}}$  acceleration level in the  $[f_{\text{lower}}, f_{\text{upper}}]$  band. The PIMS group is able to provide this type of analysis on a per-request basis.

Plot gaps (if any exist) are shown by either white or dark blue areas on the page. Care should be taken to not mistake a plot gap (represented by a blue vertical band) with a quiet period. If a plot gap exists for an entire plot (or series of successive plots), a comment is placed on the page to let the user know there is a gap in the data. These "no data available" comments will not show exact times for which the data are not available, but will only indicate missing plots.

#### Contacting PIMS

To request additional analysis or information, users are encouraged to send an e-mail to [pims@lerc.nasa.gov](mailto:pims@lerc.nasa.gov), or FAX a request to (216) 433-8660.

**Appendix D: User Comment Sheet**

We would like you to give us some feedback so that we may improve the Mission Summary Reports. Please answer the following questions and give us your comments.

1. Do the Mission Summary Reports fulfill your requirements for acceleration and mission information?  
 \_\_\_\_\_Yes \_\_\_\_\_No. If not why not?

Comments:

---



---

2. Is there additional information which you feel should be included in the Mission Summary Reports?  
 \_\_\_\_\_Yes \_\_\_\_\_No. If so what is it?

Comments:

---



---

3. Is there information in these reports which you feel is not necessary or useful?  
 \_\_\_\_\_Yes \_\_\_\_\_No. If so, what is it?

Comments:

---



---

4. Do you have internet access via: ( \_\_\_\_\_ )ftp ( \_\_\_\_\_ )WWW ( \_\_\_\_\_ )gopher ( \_\_\_\_\_ )other? Have you already accessed SAMS data or information electronically?

\_\_\_\_\_Yes \_\_\_\_\_No

Comments:

---



---

Completed by: Name: \_\_\_\_\_ Telephone \_\_\_\_\_

Address: \_\_\_\_\_ Facsimile \_\_\_\_\_

\_\_\_\_\_ E-mail addr \_\_\_\_\_

**Return this sheet to:**

**Duc Truong  
 NASA Lewis Research Center  
 21000 Brookpark Road MS 500-216  
 Cleveland, OH 44135**

**or**

**FAX to PIMS Project: 216-433-8660  
 e-mail to: pims@lerc.nasa.gov.**